

Supporting Information

Shedding Light on the Photoisomerization Pathway of Donor–Acceptor Stenhouse Adducts

Mariangela Di Donato,^{||, #, §, °} Michael M. Lerch,^{†, °} Andrea Lapini,^{||, §} Adèle D. Laurent,[∇] Alessandro Iagatti,^{||, #} Laura Bussotti,^{||} Svante P. Ihrig,[†] Miroslav Medved',^{⊗, ¶} Denis Jacquemin,^{∇, ♦} Wiktor Szymański,^{‡, †} Wybren Jan Buma,[^] Paolo Foggi,^{||, #, ⊥} Ben L. Feringa^{*, †}

† Centre for Systems Chemistry, Stratingh Institute for Chemistry, University of Groningen, Nijenborgh 4, 9747 AG, Groningen, The Netherlands

‡ Department of Radiology, University of Groningen, University Medical Center Groningen, Hanzeplein 1, 9713 GZ, Groningen, The Netherlands

|| European Laboratory for Non Linear Spectroscopy (LENS), via N. Carrara 1, 50019 Sesto Fiorentino, Italy

Istituto Nazionale di Ottica, Largo Fermi 6, 50125 Firenze, Italy

§ Dipartimento di Chimica “Ugo Schiff”, Università di Firenze, via della Lastruccia 13, 50019 Sesto Fiorentino, Italy

⊥ Dipartimento di Chimica, Università di Perugia, via Elce di Sotto 8, 06100 Perugia, Italy

∇ CEISAM, UMR CNRS 6230, BP 92208, 2 Rue de la Houssinière, 44322 Nantes, Cedex 3, France

⊗ Regional Centre of Advanced Technologies and Materials, Department of Physical Chemistry, Faculty of Science, Palacký University in Olomouc, 17. listopadu 1192/12, CZ-771 46 Olomouc, Czech Republic

¶ Department of Chemistry, Faculty of Natural Sciences, Matej Bel University, Tajovského 40, SK-97400 Banská Bystrica, Slovak Republic

♦ Institut Universitaire de France, 103 bd St Michael, 75005 Paris Cedex 5, France

^ Van't Hoff Institute for Molecular Sciences, University of Amsterdam, Science Park 904, 1098XH Amsterdam, The Netherlands.

Corresponding Author

*b.l.feringa@rug.nl

Author Contributions

° These authors contributed equally.

Table of Contents

1	Materials and Methods	3
1.1	UV/visible static and steady state measurements	3
1.2	Visible transient absorption measurements	3
1.3	Infrared transient absorption measurements.....	4
1.4	Low-temperature measurements	4
1.5	Data analysis.....	5
2	Synthesis and Characterization.....	6
3	UV/vis Absorption Spectra and Photoswitching	8
3.1	Dichloromethane	8
3.2	Chloroform	11
4	Time-Resolved Spectroscopy	14
4.1	Toluene.....	14
4.2	Chloroform	14
4.3	Dichloromethane	17
4.4	Target analysis for DASA 1	18
4.5	FTIR of open form (DASA 1).....	20
4.6	FTIR of open and closed form (DASA 2).....	21
4.7	Comparison between kinetic traces measured in the visible and IR spectral regions DASA 1 22	
4.8	Comparison between kinetic traces measured in the visible and IR spectral regions DASA 2 22	
5	Low Temperature Measurements (DASA 2).....	23
6	Computational Studies	26
6.1	Thermodynamic stability of the reaction species in their ground and excited states	26
6.2	Simulations of the long-lasting components of the IR EADS spectra.....	29
6.3	Vertical excitation energies and electronic density differences (EDD).....	33
6.4	Cartesian coordinates of various forms of compounds 1 and 2	35
7	¹ H- and ¹³ C-NMR Spectra	47
7.1	Compound S1	47
7.2	Compound 1	48
7.3	Compound S2	49
7.4	Compound 2	50

1 Materials and Methods

General reagent information: Preparation of commercially unavailable compounds: unless stated otherwise, all reactions were carried out in oven- and flame-dried glassware using standard Schlenk techniques and were run under nitrogen atmosphere. The reaction progress was monitored by Thin-layer chromatography (TLC). Starting materials, reagents and solvents were purchased from *Sigma–Aldrich*, *Acros*, *Fluka*, *Fischer*, *TCl*, *J.T. Baker* or *Macron* and were used as received, unless stated otherwise. Solvents for the reactions were of quality puriss., p.a.. Anhydrous solvents were purified by passage through solvent purification columns¹ (MBraun SPS-800). For aqueous solutions, deionized water was used. Furfural and diethylamine were purchased from Sigma Aldrich. 5-Methoxyindole and 2,2-dimethyl-1,3-dioxane-4,6-dione were purchased from Combi Blocks.

General considerations: Thin-layer chromatography analyses were performed on commercial Kieselgel 60 F₂₅₄ silica gel plates with fluorescence-indicator UV₂₅₄ (*Merck*, TLC silica gel 60 F₂₅₄). For detection of components, UV light at $\lambda = 254$ nm or $\lambda = 365$ nm was used. Alternatively, oxidative staining using aqueous basic potassium permanganate solution (KMnO₄) or aqueous acidic cerium phosphomolybdic acid solution (Seebach's stain²) was used. Drying of solutions was performed with MgSO₄ and volatiles were removed with a rotary evaporator.

General analytical information: Nuclear Magnetic Resonance spectra were measured with an Agilent Technologies 400-MR (400/54 Premium Shielded) spectrometer (400 MHz). All spectra were measured at room temperature (22–24 °C). Chemical shifts for the specific NMR spectra were reported relative to the residual solvent peak [in ppm; CDCl₃: $\delta_{\text{H}} = 7.26$; CDCl₃: $\delta_{\text{C}} = 77.16$; *d*₆-DMSO: $\delta_{\text{H}} = 2.50$; *d*₆-DMSO: $\delta_{\text{C}} = 39.52$; CD₃CN: $\delta_{\text{H}} = 1.94$; CD₃CN: $\delta_{\text{C}} = 1.32, 118.26$].³ The multiplicities of the signals are denoted by *s* (singlet), *d* (doublet), *t* (triplet), *q* (quartet), *m* (multiplet), *br* (broad signal), *app* (apparent). All ¹³C-NMR spectra are ¹H-broadband decoupled.

High-resolution mass spectrometric measurements were performed using a Thermo scientific LTQ OrbitrapXL spectrometer with ESI ionization. The molecule-ion M⁺, [M + H]⁺ and [M – X]⁺, respectively, are given in *m/z*-units. Melting points were recorded using a Stuart analogue capillary melting point SMP11 apparatus.

1.1 UV/visible static and steady state measurements

For spectroscopic measurements, solutions in Uvasol[®] grade solvents were measured in a 10 mm quartz cuvette, unless stated otherwise. UV/vis absorption spectra were recorded on an Agilent 8453 UV/vis, a Hewlet-Packard HP 8543 diode array or an Analytik Jena Specord S600 diode array. Temperature-control was exerted through a Peltier based temperature controlled cuvette holder (QuantumNorthwest). A non-coherent white light-source was purchased from Thorlabs (OSL1-EC). In chlorinated solvents, an optical cut-off filter (< 440 nm, SCF-50S-44Y) was used. The obtained UV/vis spectra were baseline corrected. Data-analysis was performed using Origin, Prism, R (<https://www.r-project.org/>) or Spectragryph software.

1.2 Visible transient absorption measurements

The apparatus used for the transient absorption spectroscopy (TAS) measurements has been described in detail before.⁴ Briefly, 100 fs pulses centred at 795 nm were produced by an integrated Ti:sapphire oscillator-regenerative amplifier system (Spectra Physics Tsunami-BMI Alpha 1000). The excitation wavelength was set at 520 nm for compound **1** (first generation DASA) and 580 nm for compound **2** (second generation DASA) and excitation power was set at 30-50 nJ for all measurements. Visible

pulses were generated by pumping a home-made non-collinear optical parametric amplifier (NOPA) with a portion of the fundamental 795 nm. The pump beam polarization has been set to magic angle with respect to the probe beam by rotating a $\lambda/2$ plate, to exclude rotational contributions. The white light probe pulse was generated by focusing a small portion of the fundamental laser radiation on a 2 mm thick sapphire window. A portion of the generated white light was sent to the sample through a different path and used as a reference signal. After passing through the sample the white light probe and reference pulses were both directed to a flat field monochromator coupled to a home-made CCD detector [<http://lens.unifi.it/ew>]. Transient signals were acquired in a time interval spanning up to 500 ps. The sample was contained in a 2 mm quartz cuvette, mounted on a movable holder in order to minimize photodegradation. Measurements were performed at room temperature. Concentrations were adjusted to an absorbance of 0.9 – 1.0 OD (for the respective optical path) at the absorption maximum which amounted to about 0.3 – 0.5 OD at excitation wavelength. Before and after the measurements, the integrity of the sample was checked on a PerkinElmer LAMBDA 950 spectrophotometer.

1.3 Infrared transient absorption measurements

The experimental setups used for time-resolved infrared measurements have been previously described.⁵ Briefly, a portion of the output of a Ti:sapphire oscillator/regenerative amplifier, operating at 1 kHz and centered at 800 nm (Legend Elite, Coherent), was split in order to generate the mid-IR probe and the Visible (VIS) pump. The infrared beam was generated by pumping a home built optical parametric amplifier (OPA) with difference frequency generation. The output of the OPA was split into two beams of equal intensity, which were respectively used as probe and reference. Broadband visible pulses were obtained by a pumping home-made non-collinear optical parametric amplifier (NOPA). The wavelength used for transient measurements were selected using appropriate cut-off filters. The polarization of the pump beam was set to magic angle with respect to the probe beam by rotating a $\lambda/2$ plate. Time resolved spectra were acquired within a time interval spanning from -5 to 300 ps. After the sample, both probe and reference were spectrally dispersed in a spectrometer (TRIAX 180, HORIBA JobinYvon) and imaged separately on a 32 channels double array HgCdTe detector (InfraRed Associated Inc., Florida USA). In order to obtain the complete transient infrared spectrum in the 1100-1700 cm^{-1} region six spectral windows were separately recorded and then overlapped. The sample cell consisted of two calcium fluoride windows separated by a Teflon spacer of 100 μm . FTIR spectra were recorded in the same cell used for transient measurements using a Bruker Alpha-T. Integrity of the sample was checked before and after the transient measurements. All measurements were performed at room temperature, except for those described in section 5, which were performed at 233 K.

1.4 Low-temperature measurements

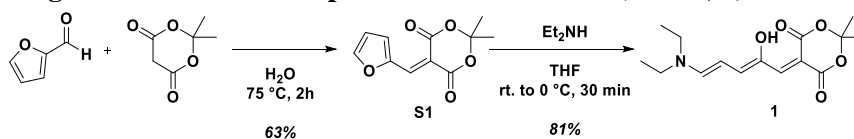
Time resolved infrared measurements at low temperature were performed using the setup described above. The sample was contained in a home-made cooling cell provided of a Peltier element. Temperatures down to 233 K could be reached at the sample position. Transient infrared spectra were recorded in the 1100-1250 cm^{-1} region upon two excitation conditions, sample **2** dissolved in deuterated dichloromethane. In the first case, the excitation wavelength was set at 580 nm, and the evolution of the excited elongated triene form of the molecule was probed in a time interval spanning up to 300 ps. In the second experiment, the sample was kept under continuous green light illumination, such as to photoaccumulate the intermediate **A'** species. The continuous source was provided by an Argon laser (LaserPhysics 300m). The photoaccumulated intermediate was pumped with a 660 nm pulse, generated from the NOPA mounted in the transient infrared setup. Transient spectra of the photoaccumulated intermediate were acquired in the same time interval used for previous measurements.

1.5 Data analysis

Femtosecond transient spectra, both in the visible and infrared spectral ranges, have been analysed by global analysis, allowing a simultaneous fit at all the acquired frequencies.⁶ The parameterization of the spectral evolution was accomplished by assuming first-order kinetics, and describing the temporal dynamics as the sum or combination of exponential functions. Global analysis was performed using the GLOTARAN package (<http://glotaran.org/>),⁷ employing a linear unidirectional “sequential” model. The number of kinetic components to be used in the global fit was determined by a preliminary singular values decomposition (*SVD*) analysis.⁸ The output of the global analysis procedure retrieved both kinetic constants and the associated spectral components (EADS, Evolution Associated Decay Spectra). In case of sample **1** an additional target analysis was performed, using the kinetic scheme depicted in Figure S4.8, producing the SADS (Species Associated Decay Spectra) depicted in Figure S4.9 and the kinetic constants reported in Table S4.4.

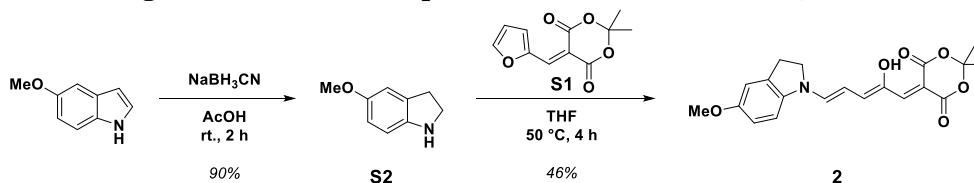
2 Synthesis and Characterization

Synthesis of first generation donor-acceptor Stenhouse adduct (DASA, 1):

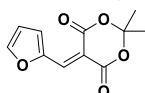


Compound **1** was synthesized according to a published procedure.^{9,10}

Synthesis of second generation donor-acceptor Stenhouse adduct (DASA, 2):

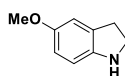


5-(furan-2-ylmethylene)-2,2-dimethyl-1,3-dioxane-4,6-dione (S1):¹⁰



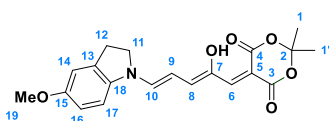
2,2-dimethyl-1,3-dioxane-4,6-dione (2.88 g, 20.0 mmol) was suspended in deionized water (60 mL). Subsequently, furfural (1.82 mL, 22.0 mmol) was added dropwise to the solution. Upon addition, the suspension was warmed to 75 °C for 2 h, until TLC indicated completion of the reaction. The reaction mixture was cooled down to room temperature. The aqueous phase was extracted with dichloromethane (3 x 50 mL). The combined organic extracts were then washed with a sat. aq. NaHSO₃-solution (100 mL), water (100 mL), sat. aq. NaHCO₃-solution (100 mL) and sat. aq. NaCl-solution (100 mL). After drying with MgSO₄, the solids were removed by filtration and the solution was concentrated under reduced pressure to obtain compound **S1** as yellow crystals in 2.80 g (63% yield). Spectral properties matched previously reported values. **Mp.** 90 - 91 °C; **¹H NMR** (400 MHz, CDCl₃) δ 1.72 (s, 6H, C(CH₃)₂), 6.71 (dd, *J* = 3.9, 1.7 Hz, 1H, ArH), 7.82 (d, *J* = 1.6 Hz, 1H, ArH), 8.29 (s, 1H, vinylH), 8.41 (d, *J* = 3.8 Hz, 1H, ArH); **¹³C NMR** (101 MHz, CDCl₃) δ 27.6, 104.5, 107.6, 115.3, 128.1, 141.1, 150.2, 150.5, 160.2, 163.2.

5-methoxyindoline (S2):¹¹



5-methoxyindoline (800 mg, 5.44 mmol) was dissolved in glacial acetic acid (50 mL). Then, sodium cyanoborohydride (1.02 g, 16.3 mmol) was added in small portions to the stirring solution at room temperature. The reaction mixture was stirred for 2 h and monitored by TLC. Upon completion of the reaction, water (4 mL) was added to the reaction mixture and all volatiles were evaporated. Aq. NaOH-solution was added to the residue (adjust to pH >9) and the aqueous phase extracted with dichloromethane (3 x 50 mL). The combined organic extracts were washed with water (100 mL) and sat. aq. NaHCO₃-solution (100 mL), then dried over MgSO₄, filtered and concentrated under reduced pressure to afford 5-methoxyindoline (**S2**, 732 mg, 90% yield) as a yellow oil. Spectral properties matched previously reported values.¹¹ **¹H NMR** (400 MHz, CDCl₃) δ 3.01 (t, *J* = 8.3 Hz, 2H, NCH₂CH₂Ar), 3.25 (s, 1H, NH), 3.54 (t, *J* = 8.3 Hz, 2H, NCH₂CH₂Ar), 3.75 (s, 3H, OCH₃), 6.61 - 6.59 (m, 2H, 2x ArH), 6.76 (s, 1H, ArH); **¹³C NMR** (101 MHz, CDCl₃) δ 30.4, 47.7, 55.8, 110.0, 111.4, 112.0, 131.0, 145.3, 153.4; **HRMS** (ESI+) calc. for C₉H₁₂NO [M + H]⁺: 150.0913, found: 150.0913.

5-((2Z,4E)-2-hydroxy-5-(5-methoxyindolin-1-yl)penta-2,4-dien-1-ylidene)-2,2-dimethyl-1,3-dioxane-4,6-dione (2):¹²



S1 (1.00 g, 4.50 mmol) was suspended in tetrahydrofuran (10 mL). Subsequently, 5-methoxyindoline (**S2**, 671 mg, 4.50 mmol) was added to the suspension at room temperature. The reaction mixture was heated to 50 °C for 4 h. Upon completion of the reaction as assessed by TLC, the reaction mixture was cooled down to room temperature and then further to -20 °C for 30 min. The formed blue precipitate was filtered off and washed thoroughly with cold diethyl ether (5 x 30 mL) and cold pentane (5 x 30 mL) to yield dark blue crystals (776 mg, 46% yield). **Mp.** gradual decomposition above 160 °C; ¹H NMR (400 MHz, DMSO-*d*₆) δ 1.62 (s, 6H, C(CH₃)₂), 3.27 (t, *J* = 7.7 Hz, 2H, NCH₂CH₂Ar), 3.78 (s, 3H, OCH₃), 4.28 (t, *J* = 7.6 Hz, 2H, NCH₂CH₂Ar), 6.16 (app t, *J* = 12.2 Hz, 1H, vinylH), 6.77 (s, 1H, vinylH), 6.96 (dd, *J* = 8.8, 2.6 Hz, 1H, Ar-H), 7.02 (d, *J* = 2.4 Hz, 1H, Ar-H), 7.15 (dd, *J* = 12.8, 1.5 Hz, 1H, vinylH), 7.52 (d, *J* = 8.9 Hz, 1H, Ar-H), 8.58 (d, *J* = 11.7 Hz, 1H, vinylH), 11.38 (d, *J* = 1.3 Hz, 1H, OH). ¹³C NMR (101 MHz, DMSO-*d*₆) δ 26.1 (**1**, **1'**), 27.3 (**12**), 49.8 (**11**), 55.7 (**19**), 87.9 (**5**), 102.6 (**2**), 106.3 (**9**), 111.2 (**14**), 112.8 (**17**), 114.2 (**16**), 133.9 (**6**), 134.8 (**13**), 136.2 (**18**), 144.4 (**7**), 148.1 (**10**), 150.6 (**8**), 158.8 (**15**), 163.8 (**3/4**), 166.5 (**3/4**); formation of some **B** within the time-course of the ¹³C-NMR experiment. **HRMS** (ESI+) calc. for C₂₀H₂₂NO₆ [M + H]⁺: 372.1442, found: 372.1415.

Matches previously reported values¹²

¹H NMR (400 MHz, CDCl₃) δ 1.73 (s, 6H, C(CH₃)₂), 3.30 (t, *J* = 8.0 Hz, 2H, NCH₂CH₂Ar), 3.82 (s, 3H, OCH₃), 4.13 (t, *J* = 7.9 Hz, 2H, NCH₂CH₂Ar), 6.15 (app t, *J* = 12.3 Hz, 1H, vinylH), 6.71 (d, *J* = 12.3 Hz, 1H, vinylH), 6.83 (d, *J* = 8.2 Hz, 1H, ArH), 6.84 (s, 1H, vinylH), 7.04 (d, *J* = 8.5 Hz, 1H, ArH), 7.25 (s, 1H), 7.63 (d, *J* = 12.5 Hz, 1H, vinylH), 11.40 (s, 1H, OH).

¹H NMR (400 MHz, CD₃CN) δ 1.66 (s, 6H, C(CH₃)₂), 3.27 (t, *J* = 7.8 Hz, 2H, NCH₂CH₂Ar), 3.79 (s, 3H, OCH₃), 4.19 (t, *J* = 7.7 Hz, 2H, NCH₂CH₂Ar), 6.18 (app t, *J* = 12.3 Hz, 1H, vinylH), 6.89 (dd, *J* = 8.9, 2.5 Hz, 1H, ArH), 6.92 – 6.97 (m, 2H, vinylH, ArH), 7.02 (d, *J* = 12.7 Hz, 1H, vinylH), 7.26 (d, *J* = 8.9 Hz, 1H, ArH), 8.06 (d, *J* = 12.0 Hz, 1H, vinylH), 11.41 (s, 1H, OH).

3 UV/vis Absorption Spectra and Photoswitching

The photochemical characterization of compound **1** has in part been reported before.⁹

3.1 Dichloromethane

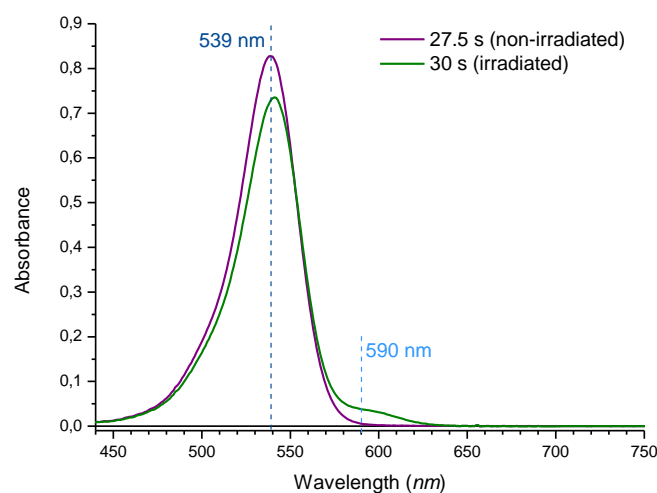
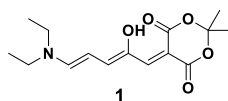


Figure S3.1 | Absorption spectra for the photoisomerization of compound **1** ($\lambda_{\text{max}} = 539 \text{ nm}$; $\sim 6 \mu\text{M}$ in dichloromethane; 293 K) at given time-points (see Figure S3.2): Photoswitching with white light (OSL1-EC).

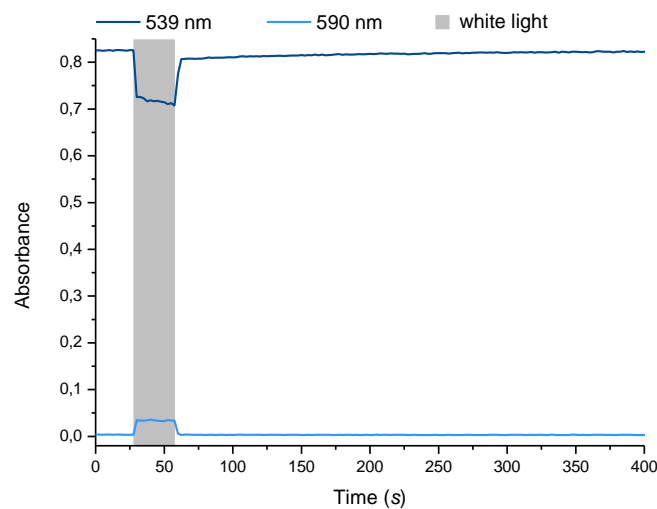


Figure S3.2 | Time-evolution of the absorption spectra from Figure S3.1 for the photoisomerization of compound **1** ($\lambda_{\text{max}} = 539 \text{ nm}$; $\sim 6 \mu\text{M}$ in dichloromethane; 293 K) with white light (OSL1-EC) observed at 539 nm and 590 nm.

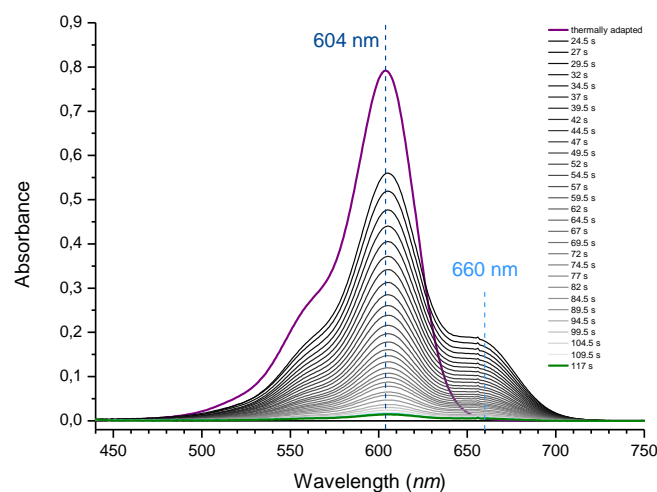
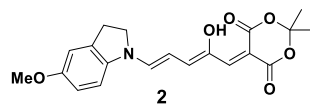


Figure S3.3 | Absorption spectra for the photoisomerization of compound **2** ($\lambda_{\text{max}} = 604 \text{ nm}$; $\sim 6 \mu\text{M}$ in dichloromethane; 293 K) at given time-points (see Figure S3.4): Photoswitching with white light (OSL1-EC).

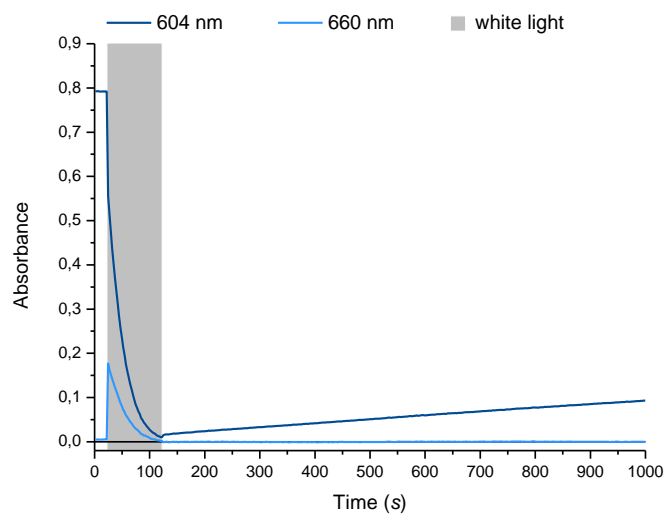


Figure S3.4 | Time-evolution of the absorption spectra from Figure S3.3 for the photoisomerization of compound **2** ($\lambda_{\text{max}} = 604 \text{ nm}$; $\sim 6 \mu\text{M}$ in dichloromethane; 293 K) with white light (OSL1-EC) observed at 604 nm and 660 nm.

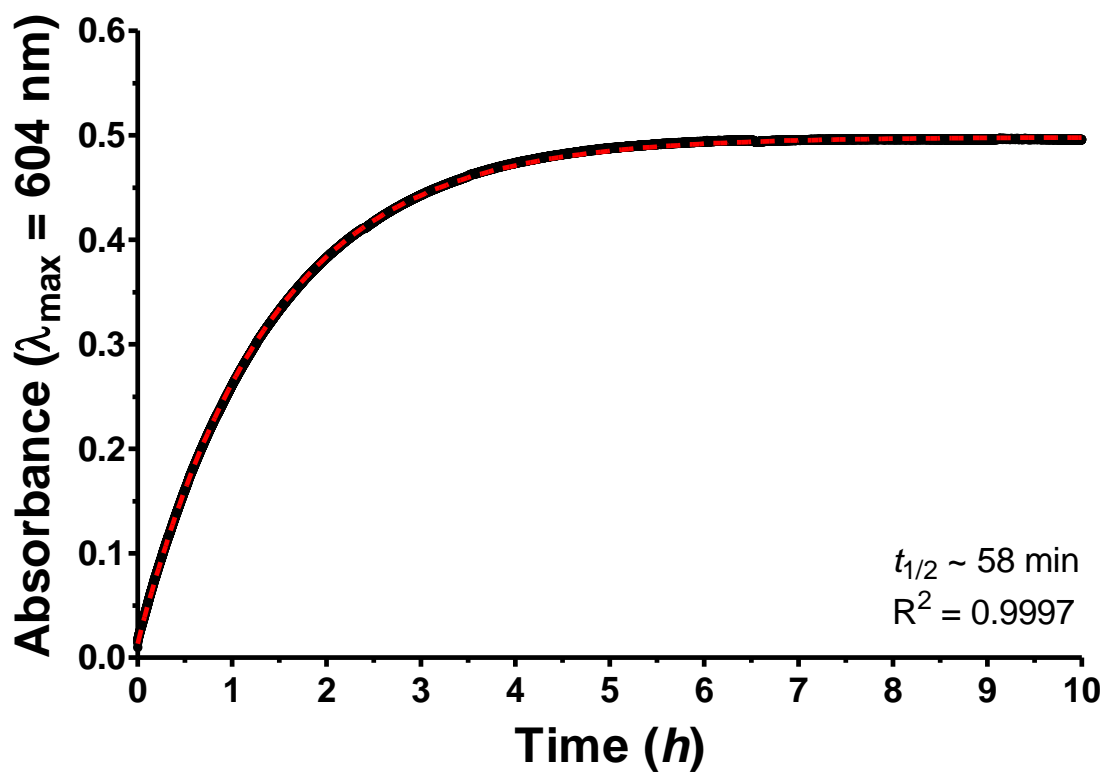


Figure S3.5 | Determination of half-life for compound 2: Points correspond to measured data (observed at $\lambda_{\max}=604$ nm, dichloromethane, $\sim 6\mu\text{M}$); line represents the fitting with single exponential process. The half-life was determined to: $t_{1/2} \sim 58$ min.

3.2 Chloroform

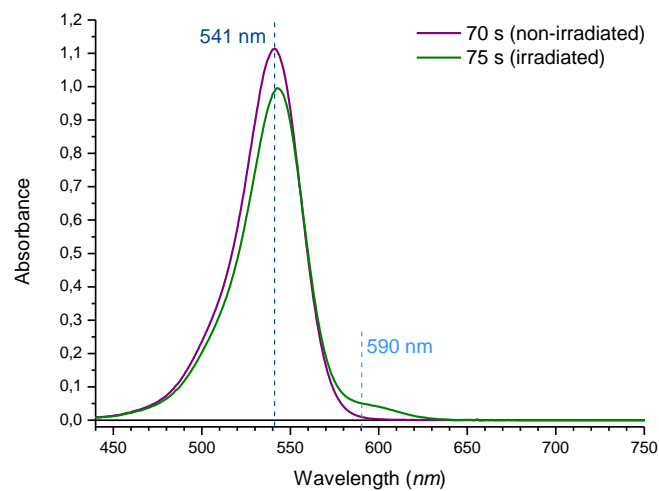
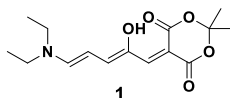


Figure S3.6 | Absorption spectra for the photoisomerization of compound **1** ($\lambda_{\max} = 541$ nm; ~ 8 μM in chloroform; 293 K) at given time-points (see Figure S3.7): Photoswitching with white light (OSL1-EC).

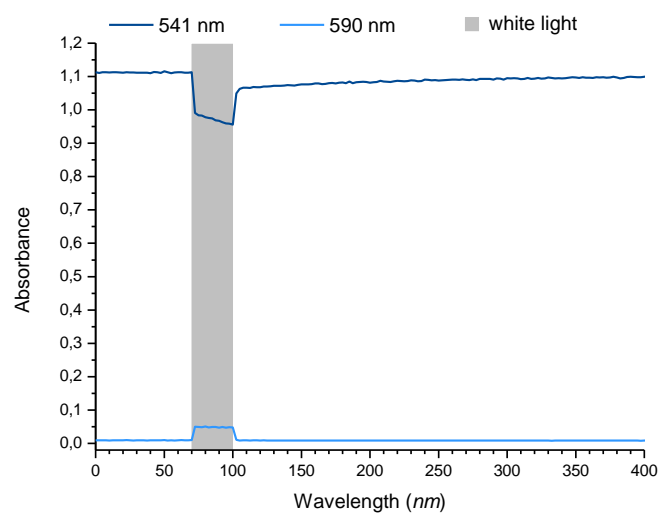


Figure S3.7 | Time-evolution of the absorption spectra from Figure S3.6 for the photoisomerization of compound **1** ($\lambda_{\max} = 541$ nm; ~ 8 μM in chloroform; 293 K) with white light (OSL1-EC) observed at 541 nm and 590 nm.

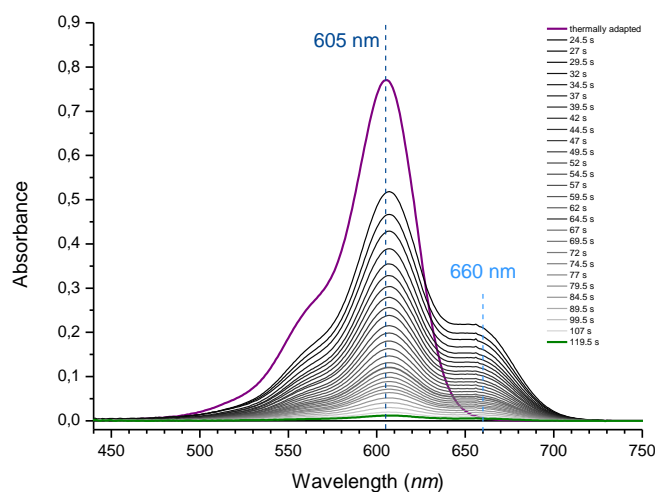
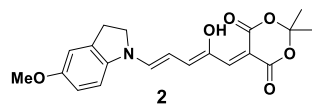


Figure S3.8 | Absorption spectra for the photoisomerization of compound **2** ($\lambda_{\text{max}} = 605 \text{ nm}$; $\sim 6 \mu\text{M}$ in chloroform; 293 K) at given time-points (see Figure S3.9): Photoswitching with white light (OSL1-EC).

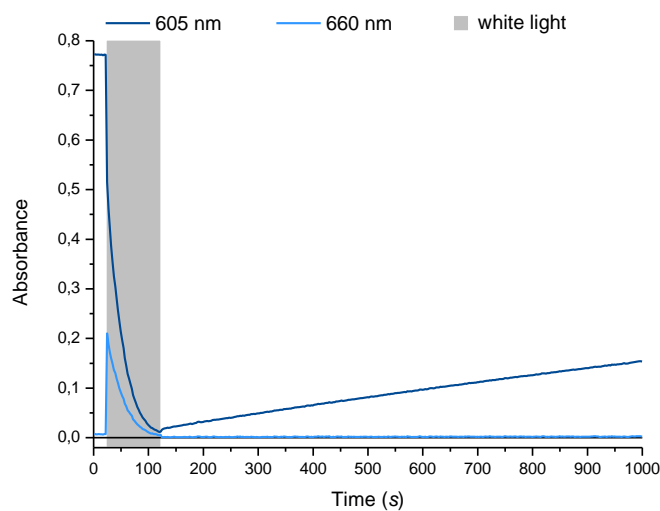


Figure S3.9 | Time-evolution of the absorption spectra from Figure S3.8 for the photoisomerization of compound **2** ($\lambda_{\text{max}} = 605 \text{ nm}$; $\sim 6 \mu\text{M}$ in chloroform; 293 K) with white light (OSL1-EC) observed at 605 nm and 660 nm.

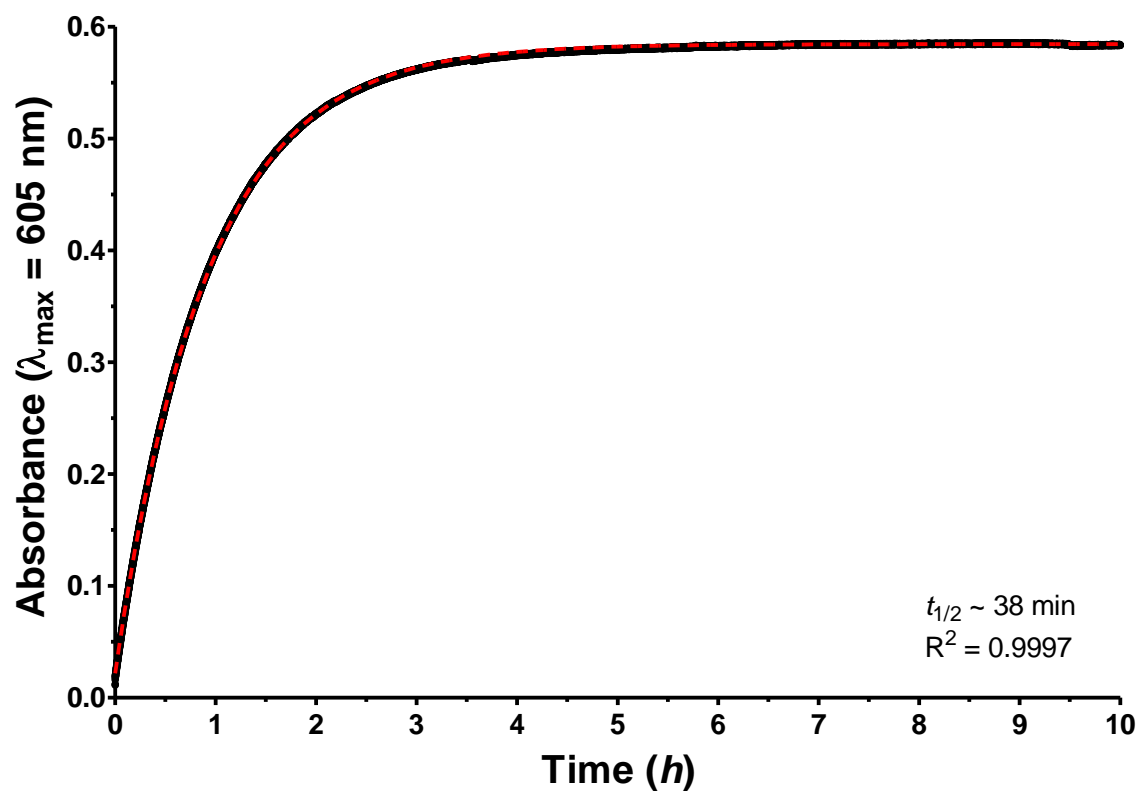


Figure S3.10 | Determination of half-life for compound **2**: Points correspond to measured data (observed at $\lambda_{\max}=605 \text{ nm}$, chloroform, $\sim 6\mu\text{M}$); line represents the fitting with single exponential process. The half-life was determined to: $t_{1/2} \sim 38 \text{ min}$.

4 Time-Resolved Spectroscopy

4.1 Toluene

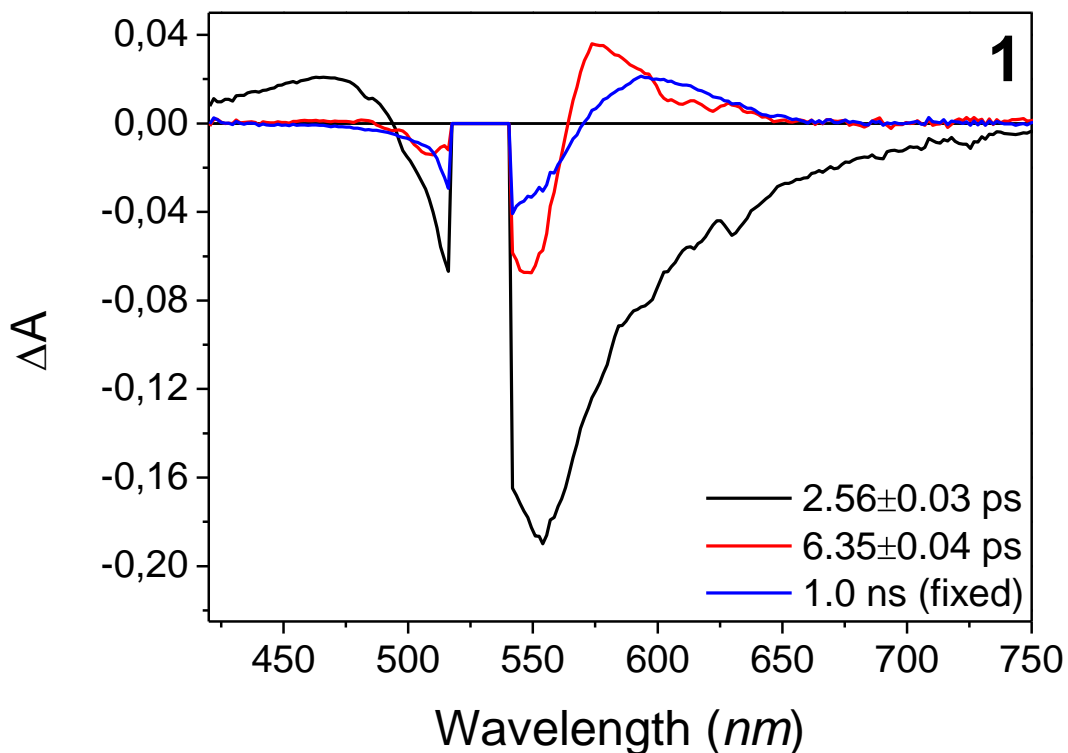


Figure S4.1 | EADS (Evolution-Associated Difference Spectra) obtained from global analysis of time resolved visible data recorded for sample **1** in toluene. Spectral range omitted due to scattering.

4.2 Chloroform

Table 4.1: Comparison of life-times associated to the measured EADS.

Entry	Measurement	τ_1 (ps)	τ_2 (ps)	τ_3
1	1 , VIS	2.21±0.02	10.0±0.3	4.76±0.01 ns
2	1 , TRIR	2.11±0.01	10.2±0.1	712±2 ps
3	2 , VIS	2.05±0.05	27.8±0.1	3.12±0.02 ns
4	2 , TRIR	2.01±0.03	24.1±0.3	537±1 ps

Table 4.2: Spectral maxima and minima associated with the measured EADS.

Entry	Compound	Excited State	EADS 1 (black)	EADS 2 (red)	EADS 3 (blue)
1	1	460 nm	537 nm	567 nm	586 nm
2	2	482 nm	610 nm	607 nm	649 nm

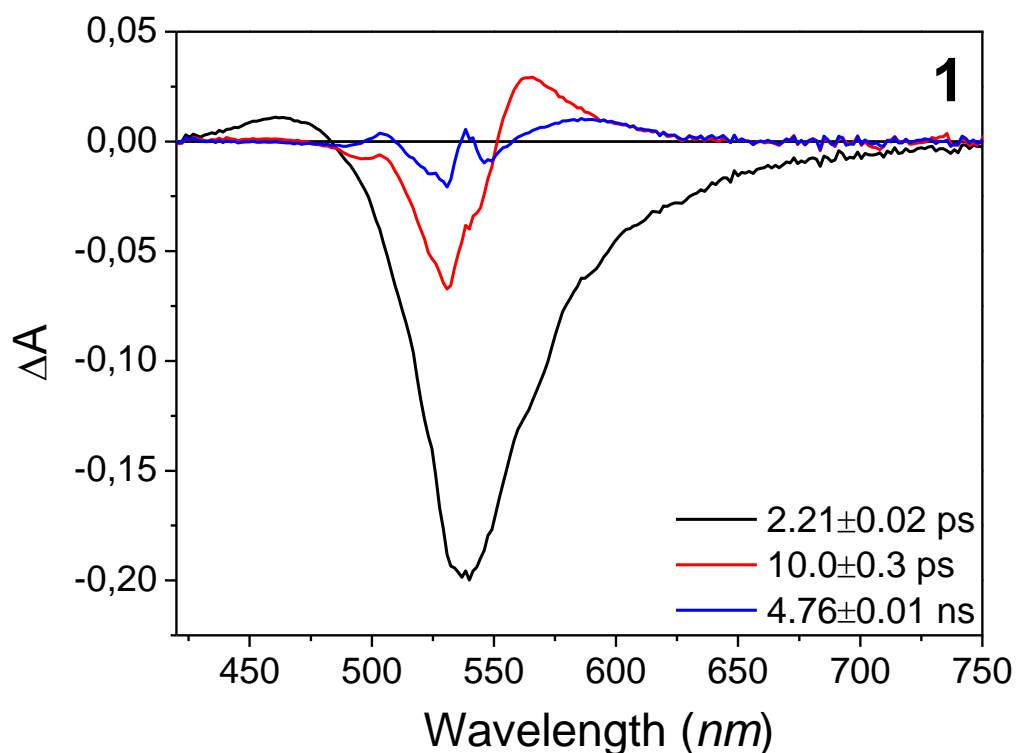


Figure S4.2 | EADS obtained from global analysis of time resolved visible data recorded for sample **1** in chloroform.

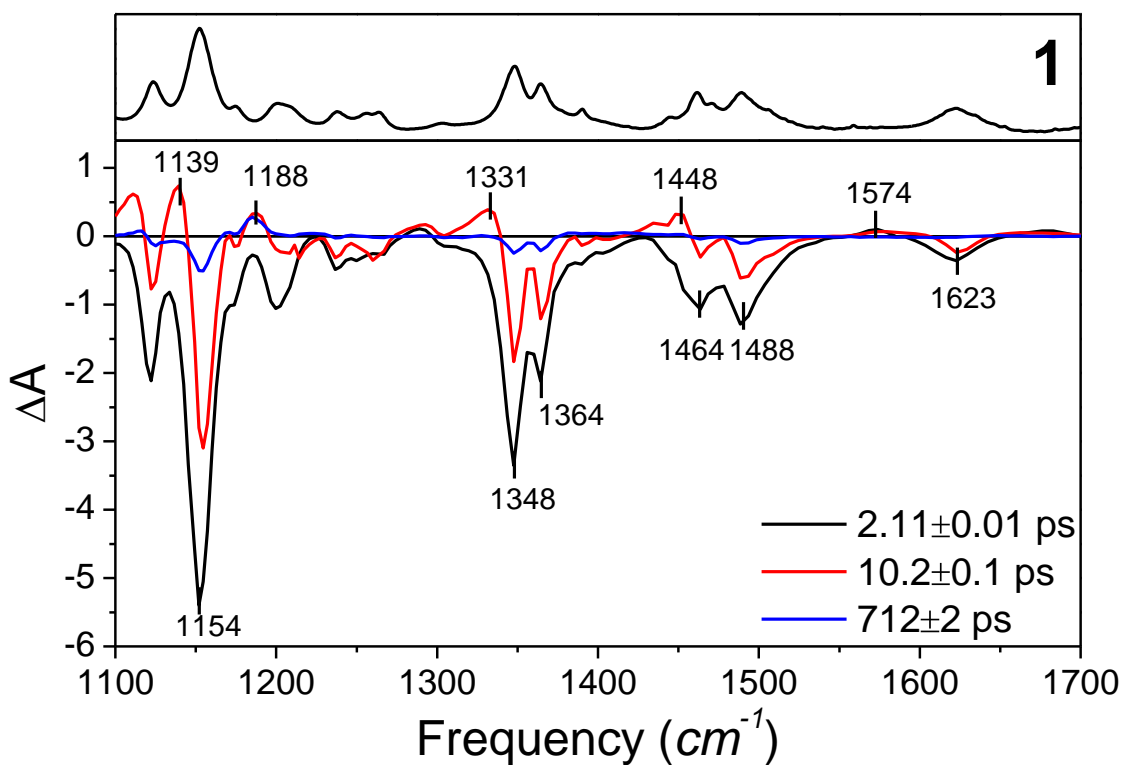


Figure S4.3 | EADS obtained from global analysis of time resolved infrared data recorded for sample **1** in chloroform. The black spectrum on top of the panel is the FTIR spectrum of the linear **A** form.

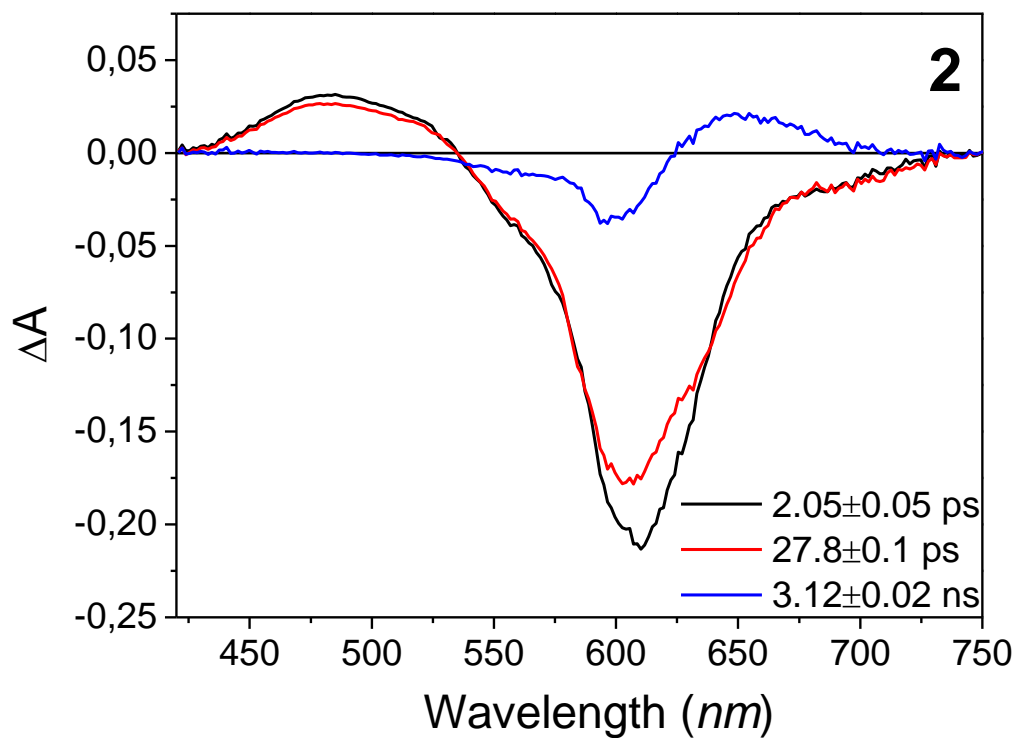


Figure S4.4 | EADS obtained from global analysis of time resolved visible data recorded for sample 2 in chloroform.

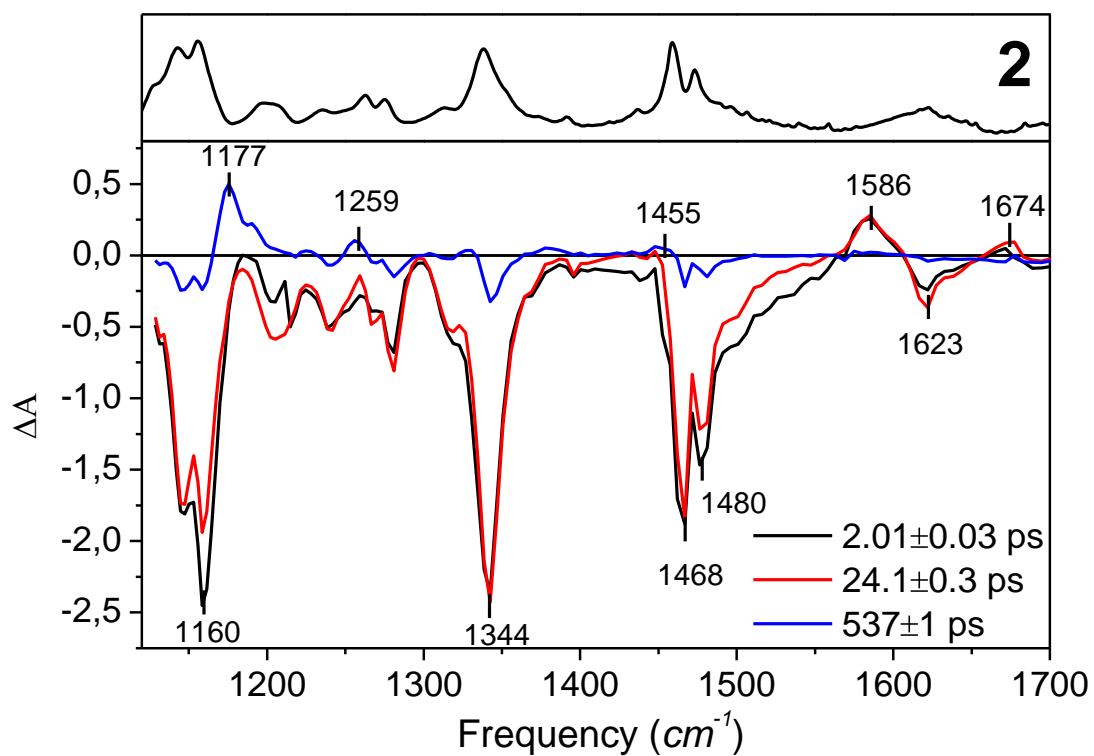


Figure S4.5 | EADS obtained from global analysis of time resolved infrared data recorded for sample 2 in chloroform. The black spectrum on top of the panel is the FTIR spectrum of the linear A form.

4.3 Dichloromethane

Table 4.3: Comparison of life-times associated to the measured EADS.

Entry	Compound	τ_1 (ps)	τ_2 (ps)	τ_3
1	1	2.10 ± 0.05	6.13 ± 0.3	1.76 ± 0.04 ns
2	2	2.11 ± 0.02	25.9 ± 0.1	1.32 ± 0.05 ns

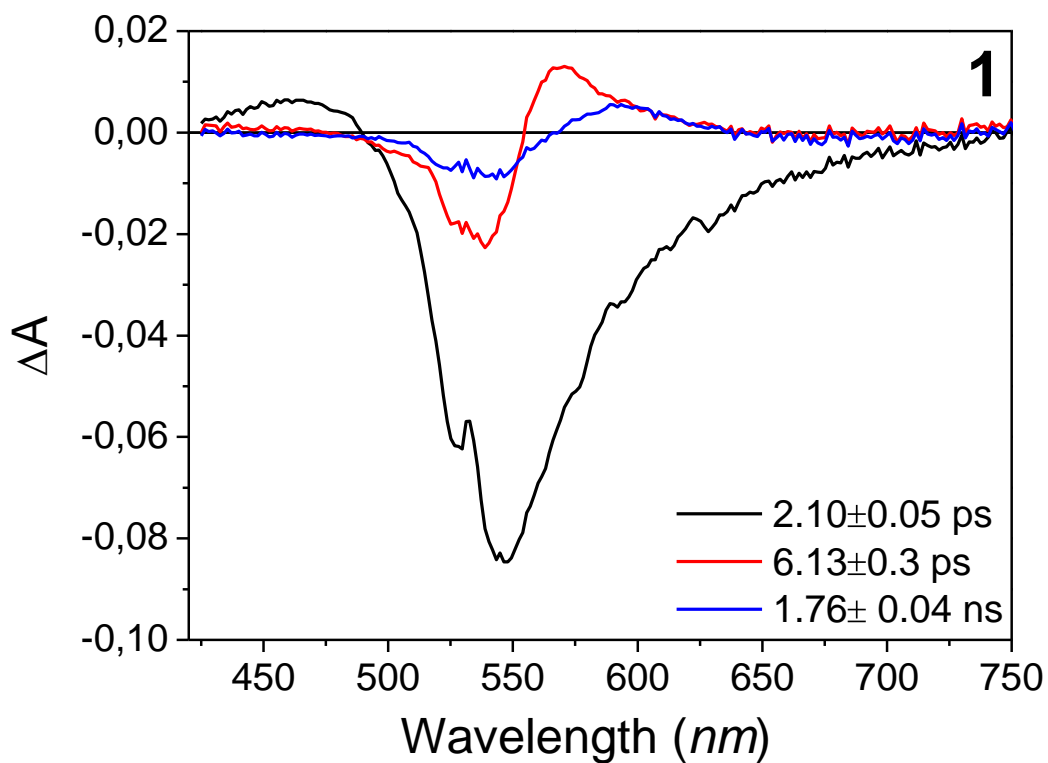


Figure S4.6 | EADS obtained from global analysis of time resolved visible data recorded for sample **1** in dichloromethane.

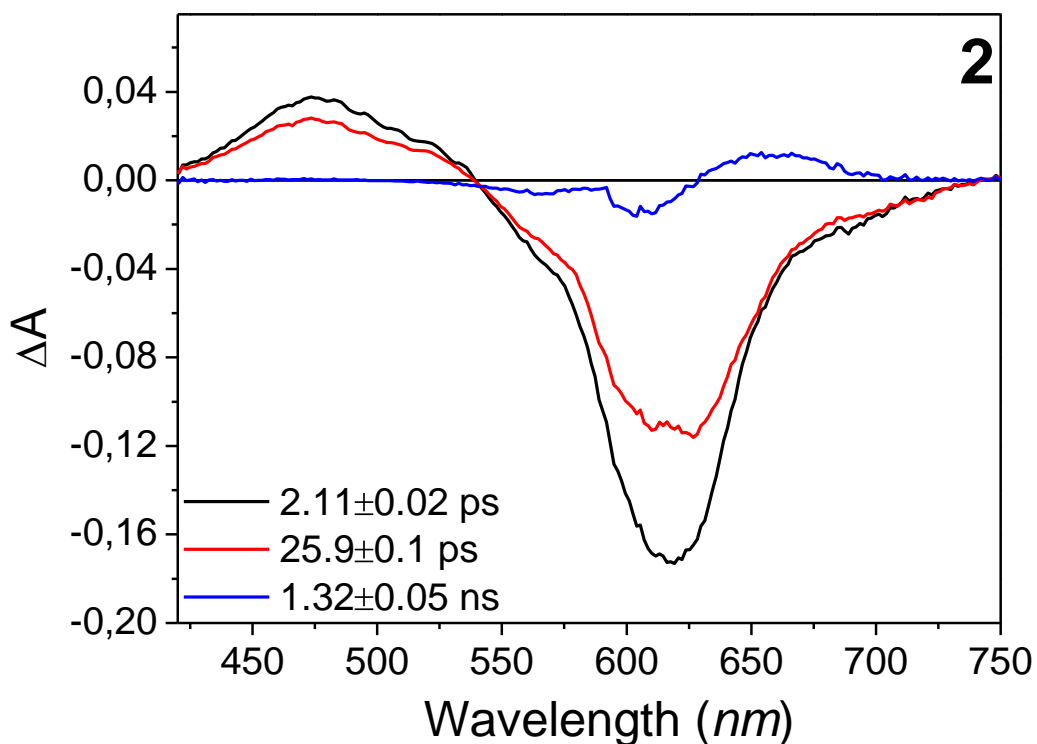


Figure S4.7 | EADS obtained from global analysis of time resolved visible data recorded for sample **2** in dichloromethane.

4.4 Target analysis for DASA 1

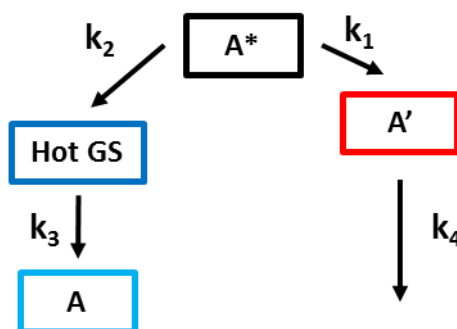
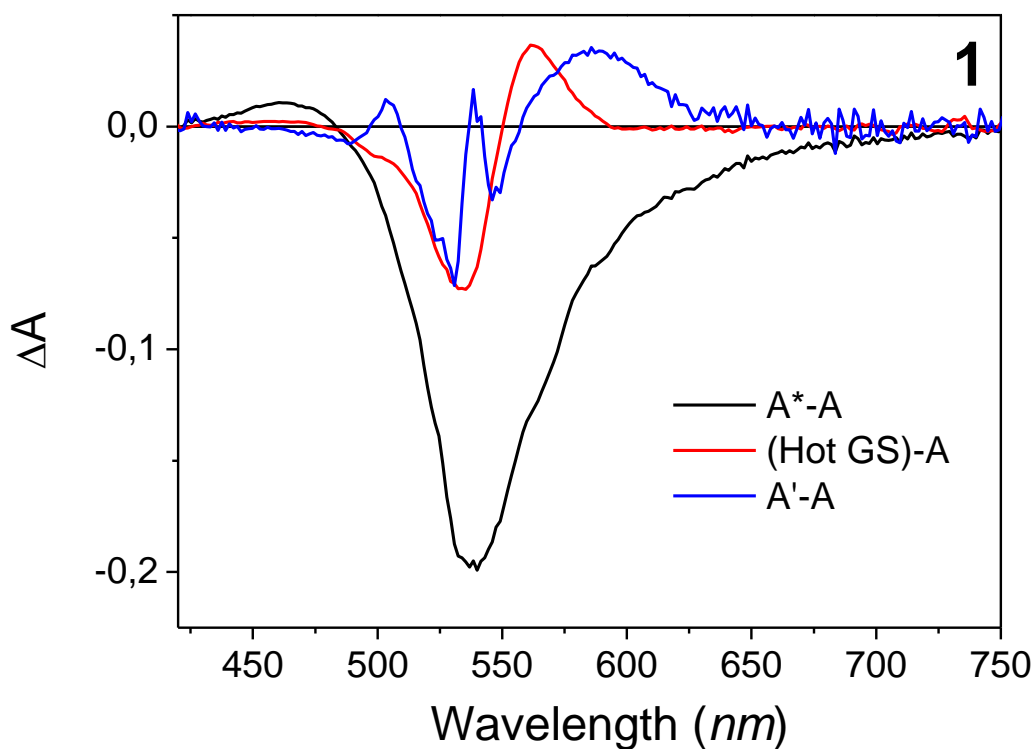


Figure S4.8 | Kinetic scheme used for target analysis of the time resolved data for sample **1** recorded both in the visible and IR spectral range.

Table 4.4: Comparison of kinetic constants associated to the Species Associated Spectra (SAS) obtained from target analysis.

Entry	Measurement	k_1 (ps ⁻¹)	k_2 (ps ⁻¹)	k_3 (ps ⁻¹)	k_4 (ps ⁻¹)
1	1, VIS	0.657	1.53	0.115	0.000259
2	1, TRIR	0.638	1.489	0.105	0.00155

a)



b)

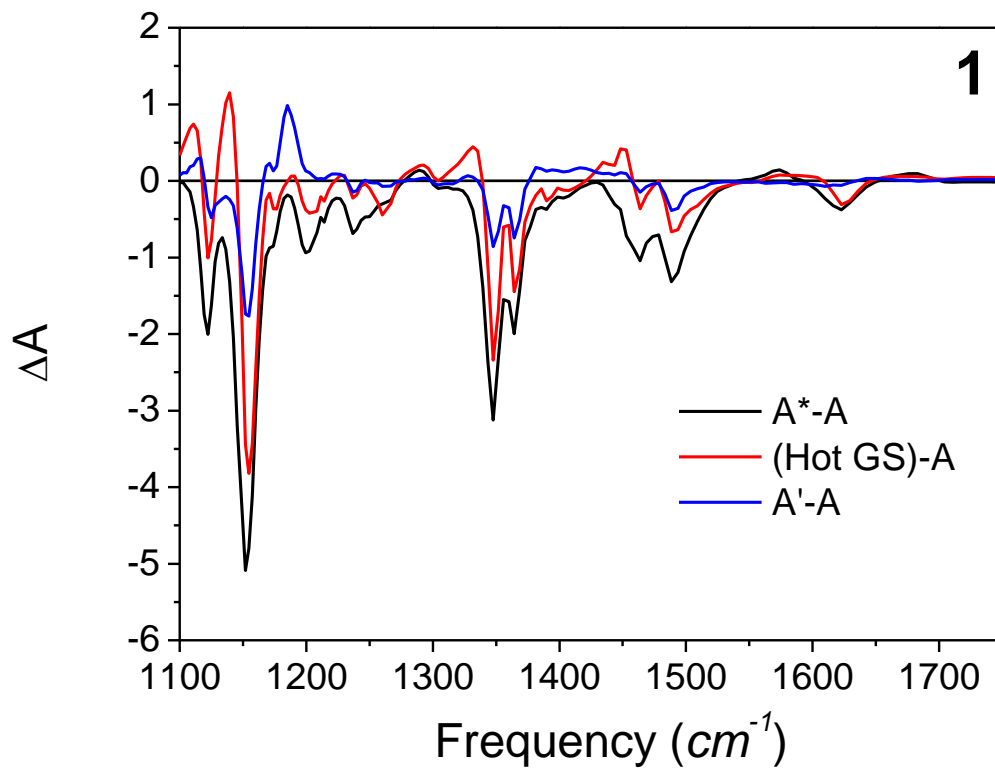


Figure S4.9 | Species Associated Spectra (SAS) retrieved from a target analysis employing the kinetic scheme depicted in Figure S4.8 of the time resolved data recorded both in the visible (a) and IR (b) spectral range for sample 1.

4.5 FTIR of open form (DASA **1**)

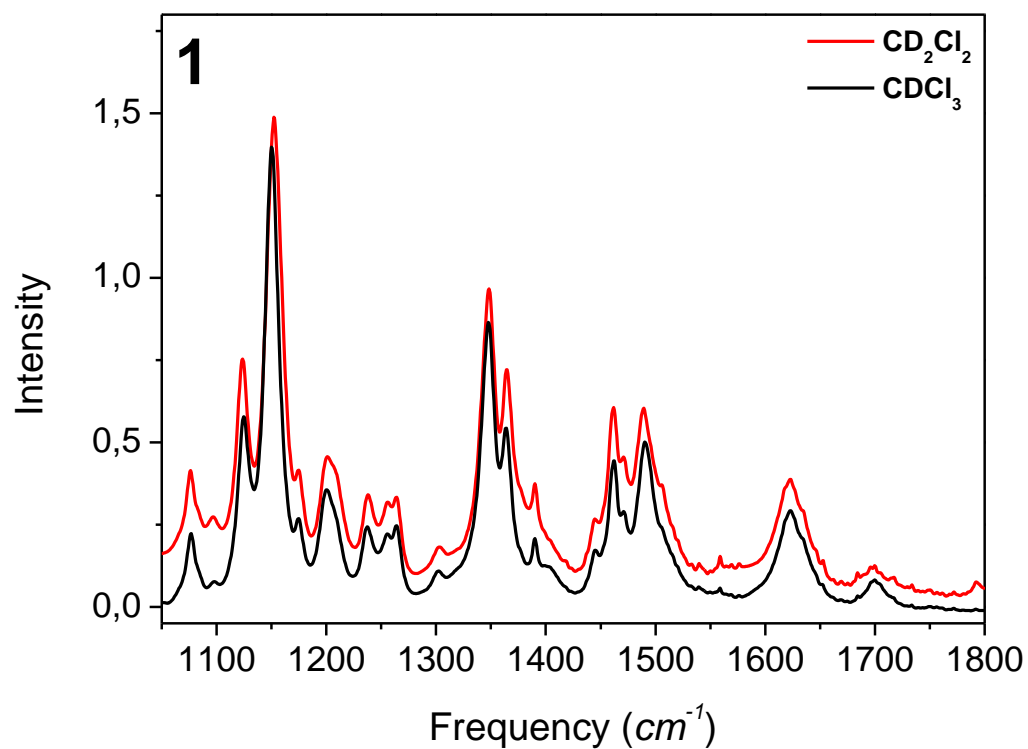


Figure S4.10 | FTIR of the open form **A** of sample **1** in CD_2Cl_2 and $CDCl_3$ (for comparison). Compound **1** does not cyclize in chlorinated solvents, thus no **B** form is shown.

4.6 FTIR of open and closed form (DASA 2)

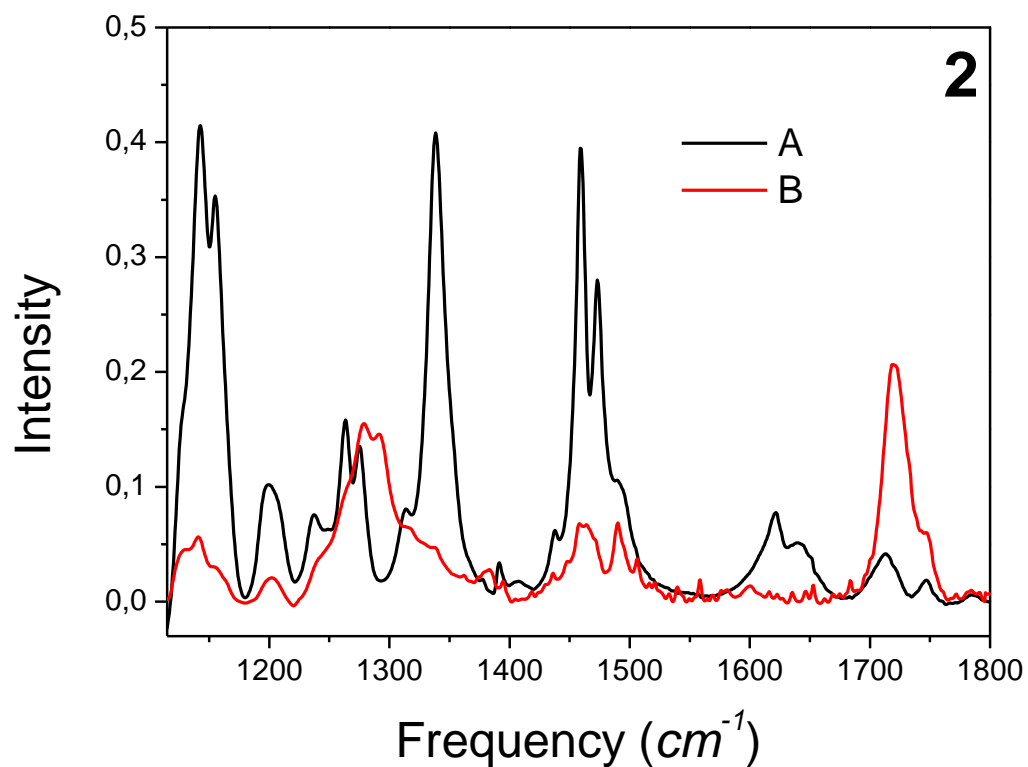


Figure S4.11 | FTIR of the open form **A** and closed form **B** of sample **2** in dichloromethane, where the molecule reversibly cyclizes with a half-life of the unstable isomer **B** of ~58 min. The closed form has been produced upon illumination with a white light source (Thorlabs, OSL1-EC). Major changes observed upon ring closure are consistent with the loss of the conjugated triene structure (intensity decreasing in the C-C and C=C stretching regions) and with the formation of a carbonyl group of the cyclopentenone structure (intensity increasing at 1730 cm^{-1}).

4.7 Comparison between kinetic traces measured in the visible and IR spectral regions DASA 1

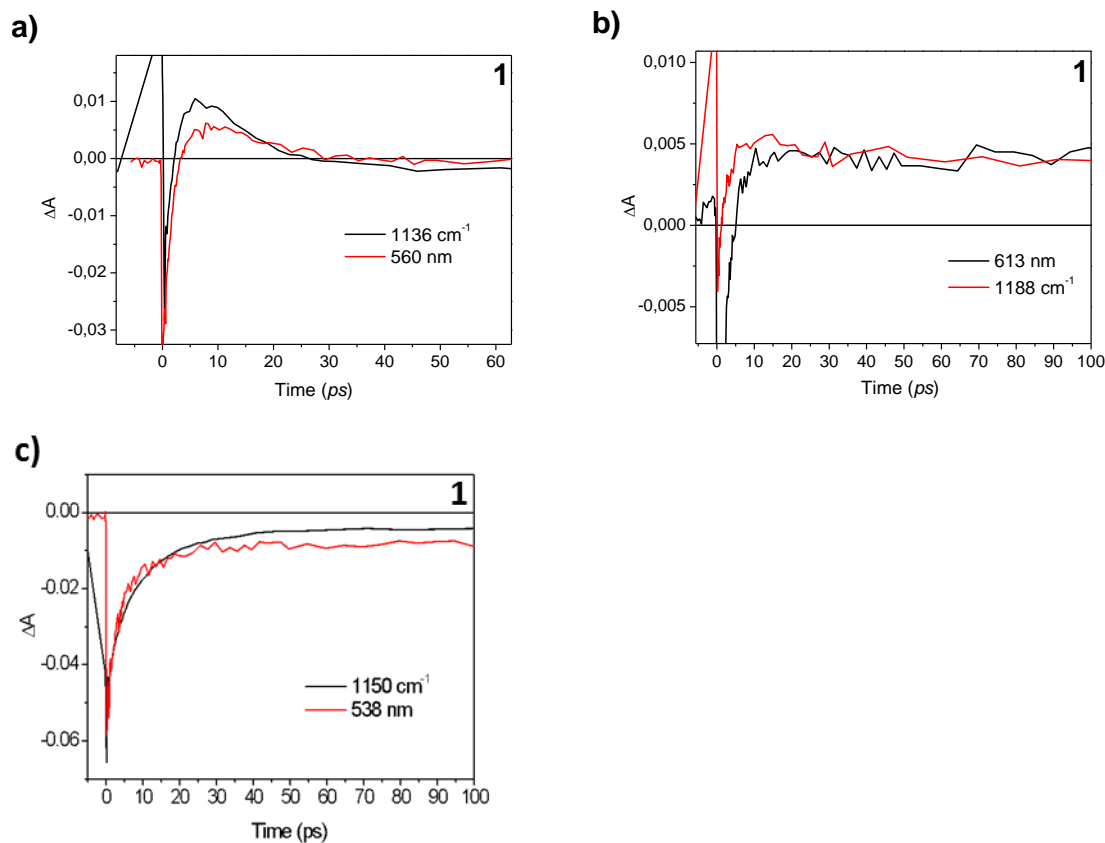


Figure S4.12 | Comparison of selected kinetic traces recorded in the visible and mid-IR spectral ranges. a) Traces most representative for the ‘fast’ evolution process; b) Kinetic traces showing the formation of the long living species; c) Kinetic traces representing the bleach recovery of the elongated form.

4.8 Comparison between kinetic traces measured in the visible and IR spectral regions DASA 2

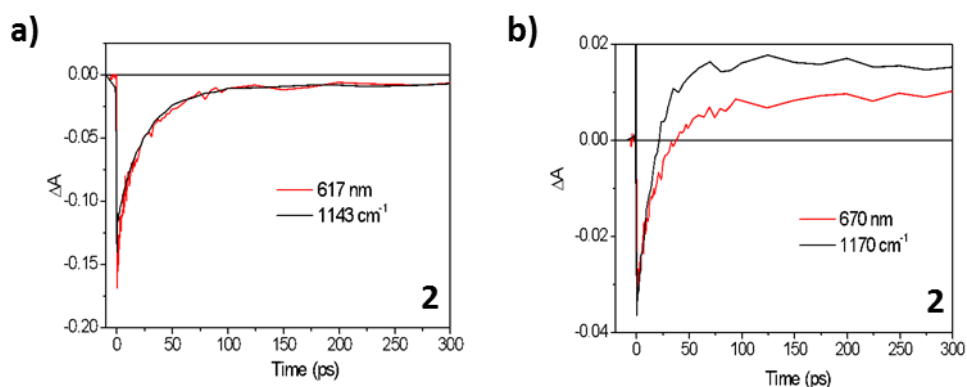
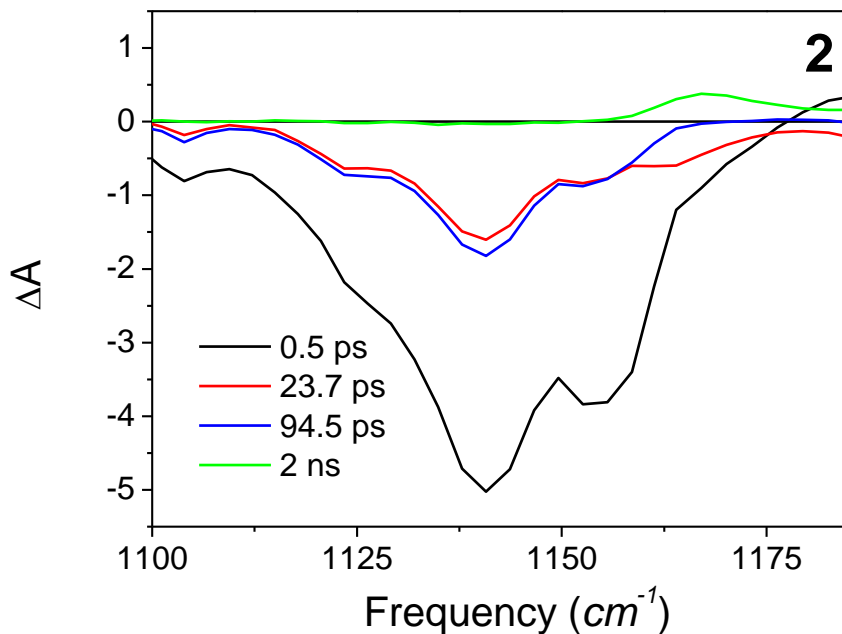


Figure S4.13 | Comparison selected kinetic traces recorded in the visible and mid-IR spectral ranges. a) Kinetic traces representing the bleach recovery of the elongated form. b) Traces showing the formation of the long living species;

5 Low Temperature Measurements (DASA 2)

a)



b)

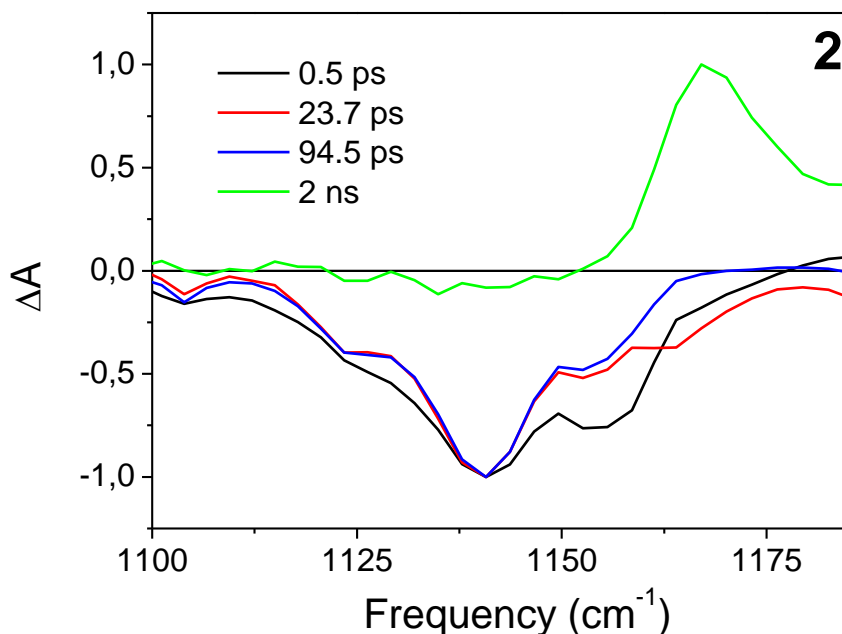


Figure S5.1 | a) EADS obtained from global analysis of kinetic traces recorded by performing a transient absorption measurement with visible excitation (centred at 580 nm) and mid-IR probe. Measurements have been performed in deuterated dichloromethane. The sample has been cooled to 233 K. The analysed spectral region is that showing the marker bands for the intermediate formation. It is evident that the reaction occurs also at low temperature, however the kinetics for the *Z-E* isomerization is slower, as evidenced by the kinetic traces comparison reported in Figure S5.3. The formation of the A' band peaked at 1167 cm^{-1} is highlighted in the normalized EADS (panel b).

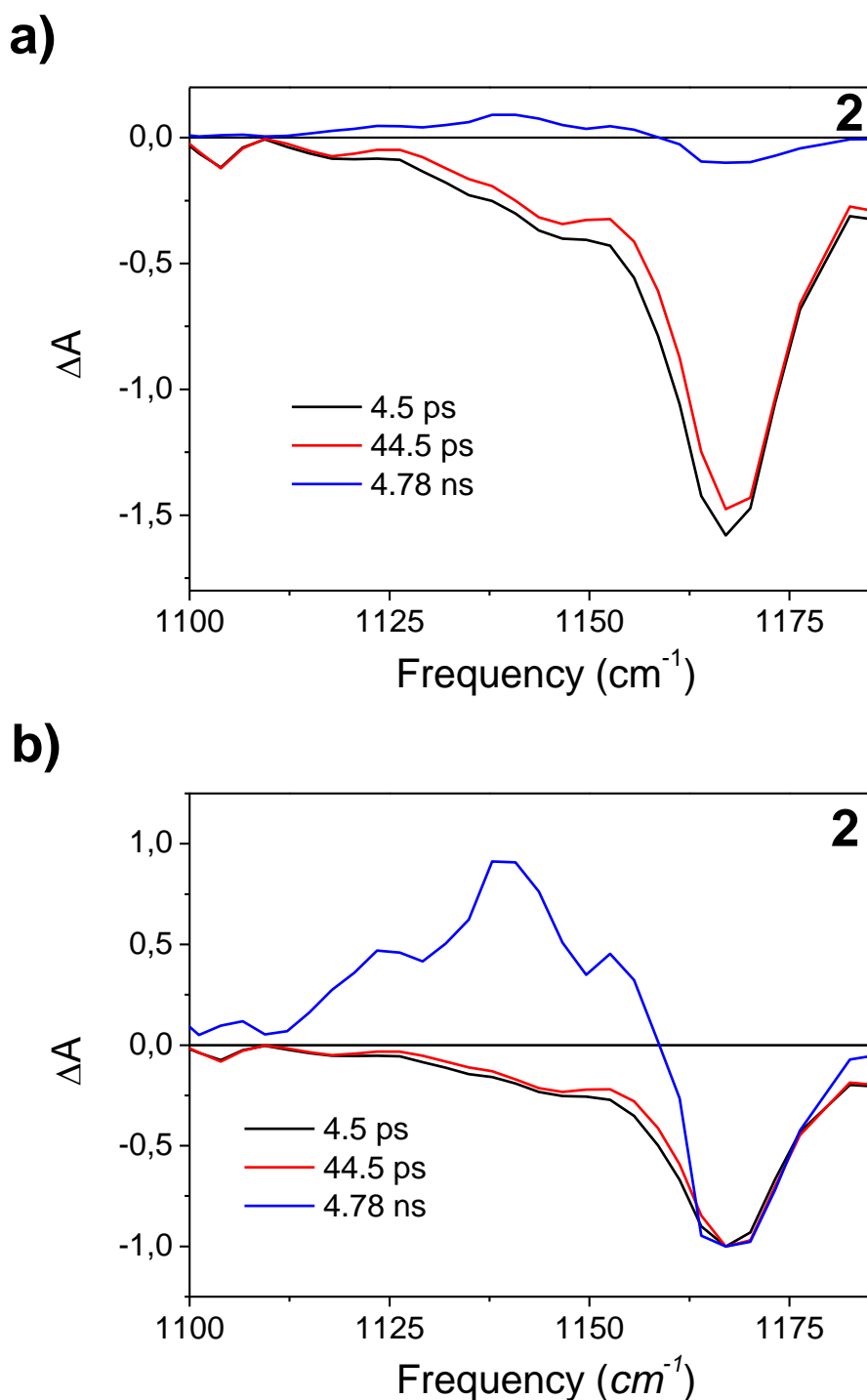


Figure S5.2 | a) EADS obtained from global analysis of kinetic traces recorded by performing a transient absorption measurement with visible excitation and mid-IR probe. Measurements have been performed in deuterated dichloromethane. The sample has been cooled to 233 K and kept under continuous green light illumination. In this way, the isomerized form is trapped and can be selectively excited. The ultrafast pump pulse has been centred at 660 nm. The analysed spectral region is again the one where the marker bands for the intermediate formation are observed. In this case, by pumping the intermediate, the recovery of the elongated form can be observed (the band of the intermediate is bleached and that of the elongated form appears with positive sign on a 44 ps timescale). The formation of the elongated form A band peaked at 1140 cm^{-1} is highlighted in the normalized EADS (panel b).

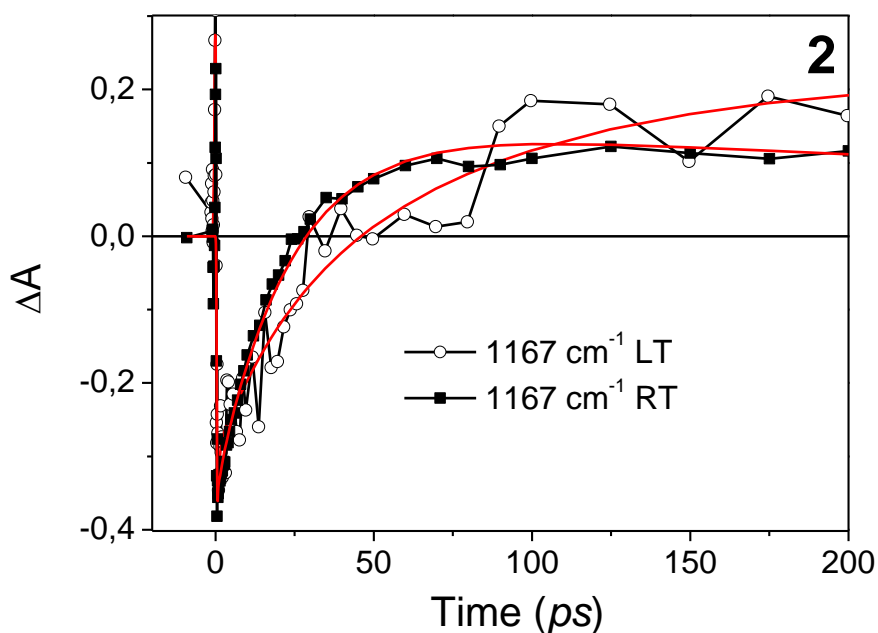


Figure S5.3 | Comparison of the kinetic traces representative for the *Z-E* isomerization (1167 cm^{-1}) recorded at room temperature (RT, black squares) and at 233 K (LT, open circles). The red lines represent the fit obtained from global analysis.

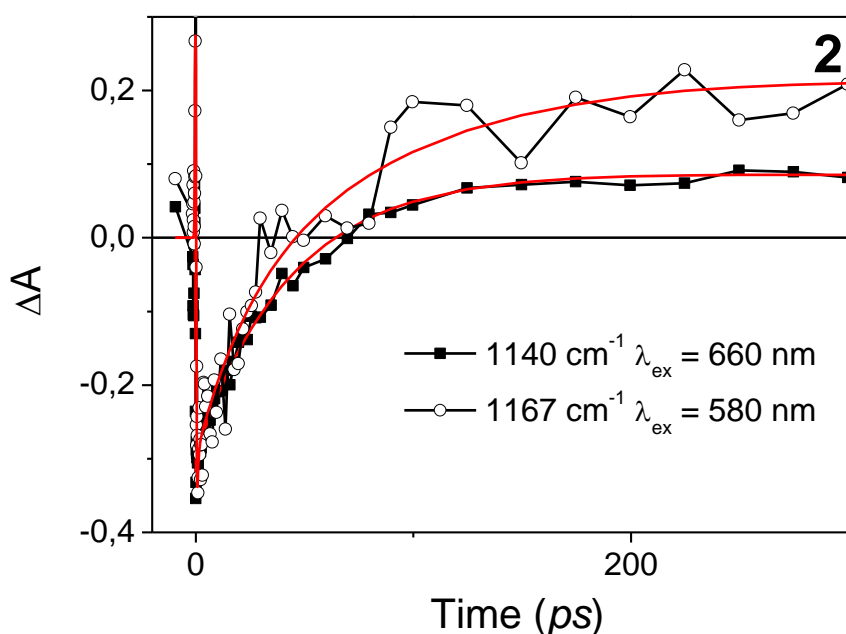


Figure S5.4 | Comparison of the kinetic traces representative for the photoreaction from the elongated to intermediate form (open circles) and from the intermediate to elongated form (black squares) obtained by pumping the sample at 233 K respectively with an ultrafast pulse centered at 660 nm (under continuous green illumination) and an ultrafast pulse centered at 580 nm (without continuous green illumination). The red lines represent the fit obtained from global analysis.

6 Computational Studies

6.1 Thermodynamic stability of the reaction species in their ground and excited states

All calculations were performed with the Gaussian09¹³ and Gaussian16¹⁴ programs. The ground state (GS) and first excited state (ES) structures of the initial elongated triene form **A** as well as those of twisted intermediate species **A'** and **A''** of both DASA generations were optimized at the M06-2X level¹⁵ using the 6-31+G(d) atomic basis set,¹⁶ since this exchange-correlation functional is known to perform well not only for the GS thermochemistry, but also in describing excited states. For comparison, we also report the energy values obtained with B3LYP/6-31++G(d,p), which was used later in the analysis of IR spectra. All minima were checked against the presence of imaginary frequencies. The solvent effects were included by using the universal continuum solvation model based on solute electron density (SMD).¹⁷ The optimized GS structures are presented in Figure S6.1. As shown in Table S6.1 and Figure S6.2, the M06-2X and B3LYP methods provide consistent results for the local minima, although the latter predicts slightly higher barriers for the single-bond rotation step.

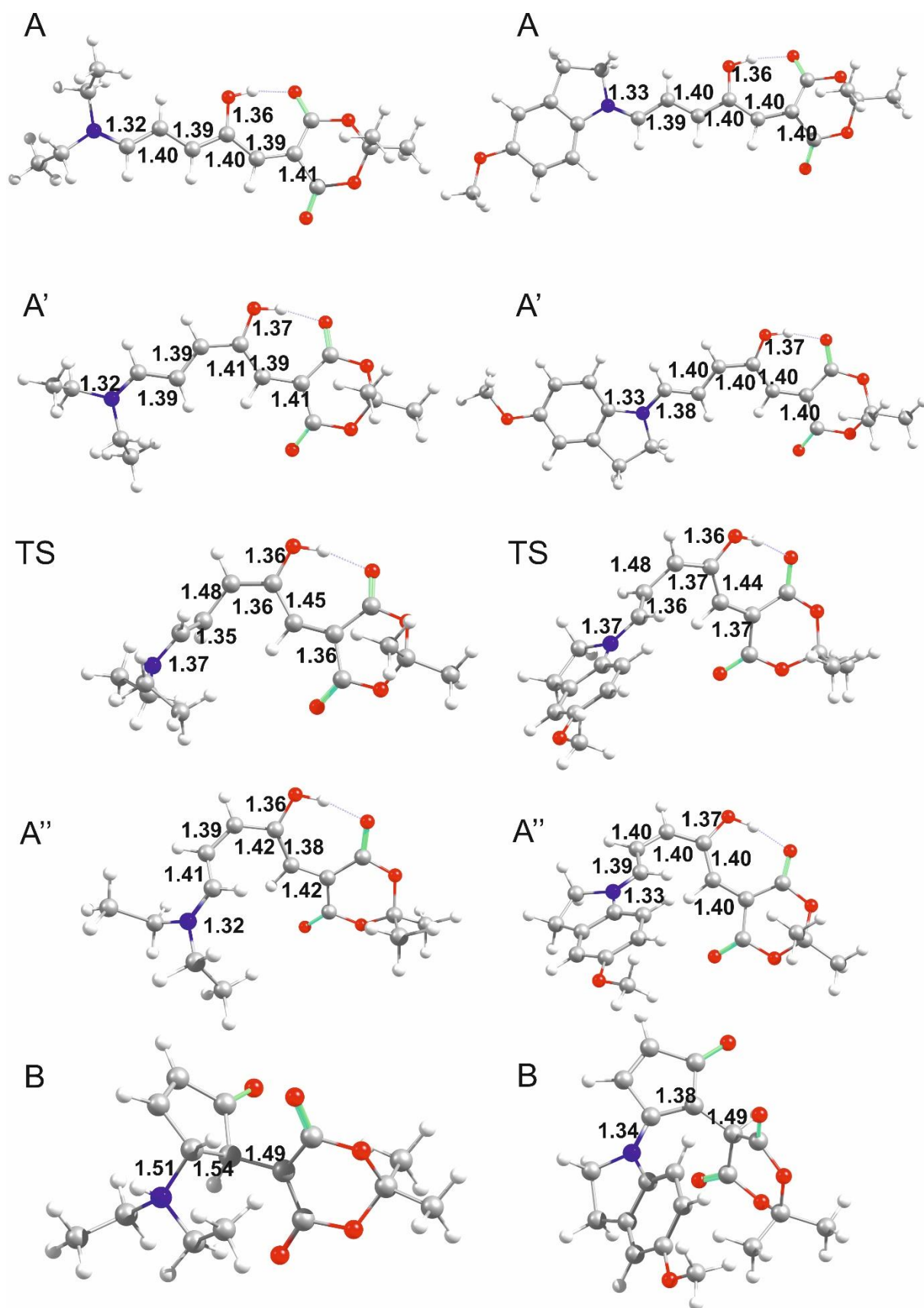


Figure S6.1 | GS structures of the initial form **A**, of the two twisted intermediate species (**A'** and **A''**), transition state (**A'**-> **A''**) and the final form **B** for DASA 1 (left) and DASA 2 (right) in chloroform. Geometries were optimized at the SMD/M06-2X/6-31+G(d) level of theory. Selected bond lengths are given in Å.

Table S6.1 | Relative electronic and Gibbs free energies (in kcal/mol) of the initial form **A**, of the two **A'** and **A''** twisted intermediate species and of the transition state relating **A'** to **A''** of **DASA 1** and **2** evaluated at the SMD/M06-2X/6-31+G(d) level of theory. For comparison, the SMD/B3LYP/6-31++G(d,p) values are reported for the ground state structures in parentheses.

System	Ground State		Excited State	
	ΔE	ΔG	ΔE	ΔG
DASA 1				
A	0.00	0.00	0.00	0.00
A'	5.26 (4.94)	4.72 (4.66)	-2.35	0.39
TS	16.5 (20.5)	15.9 (19.2)		
A''	8.45 (9.63)	9.07 (10.0)	-0.82	2.30
DASA 2				
A	0.00	0.00	0.00	0.00
A'	5.09 (4.87)	5.03 (5.16)	-1.18	1.11
TS	14.2 (18.6)	14.3 (17.7)		
A''	8.63 (9.58)	7.69 (9.93)	0.01	2.74

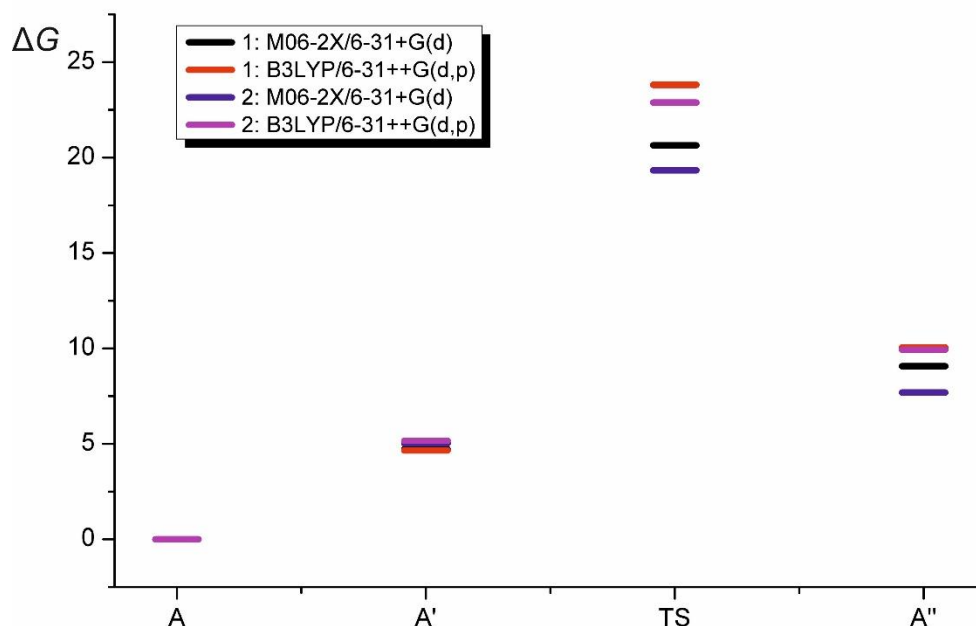


Figure S6.2 Relative Gibbs energy levels of GS structures of **1** and **2** in chloroform.

6.2 Simulations of the long-lasting components of the IR EADS spectra

For the EADS analysis of the IR spectra, the structures of **A**, **A'** and **A''** of both DASA generations have been optimized at the B3LYP level¹⁸ using the 6-31++G(d,p) basis set.¹⁹ The effects of solvent environment were incorporated at the SMD model as above. The scaled ground state IR spectra were obtained at the same level by using the scaling factor 0.98, which was selected by comparing the theoretical and experimental IR spectra of the species **A** (see Figures S6.3-6.6). In order to account for inhomogeneous broadening effects, the computed stick spectra have been convoluted by Gaussian functions with the FWHM parameter set to 12 cm^{-1} to capture the main features of the experimental spectra of the species **A**. Anharmonic IR spectra were also simulated with Gaussian16 software by applying the second-order vibrational perturbation theory (VPT2)²⁰ for selected anharmonic modes (in the $1100\text{-}1700\text{ cm}^{-1}$ range), but this approach was not found superior to the scaled harmonic approximation (see Figure S6.7). Whereas the frequencies were in large extent in good agreement with experiment, the intensities were not well reproduced, which was probably due to the (neglected) couplings with lower frequency vibration modes. Unfortunately, the full anharmonic treatment would be computationally too demanding for our systems. In Figure S6.8 we present a comparison of the experimental and simulated long-lasting component of IR EADS ($\text{GS}(\mathbf{A}') - \text{GS}(\mathbf{A})$) of DASA **2** (sample **2**) in dichloromethane (DCM) using harmonic frequencies.

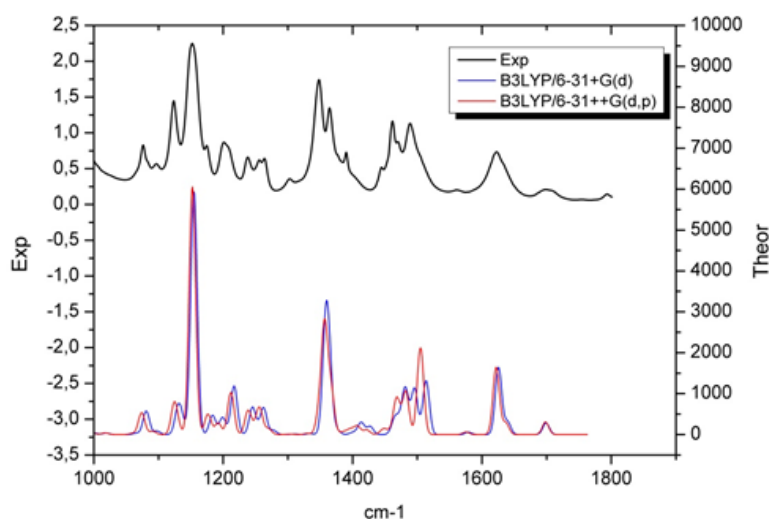


Figure S6.3 | A comparison between experimental and scaled theoretical ground state IR spectra of **A** for DASA **1** (sample **1**) in chloroform.

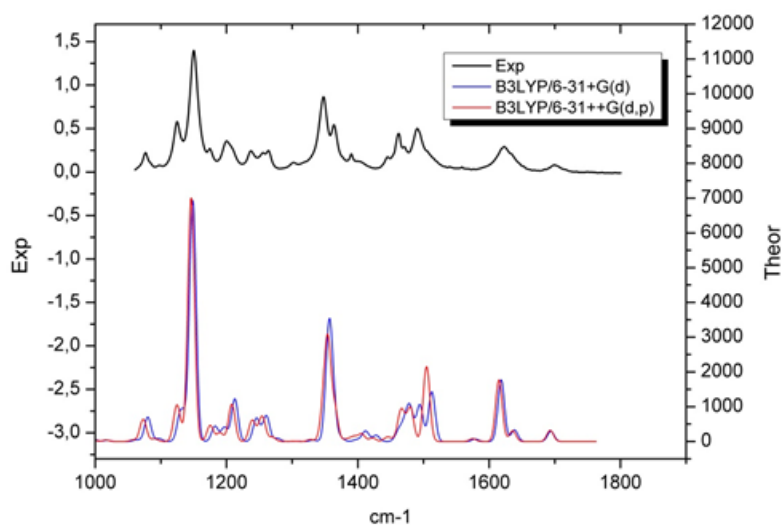


Figure S6.4 | A comparison between experimental and scaled theoretical ground state IR spectra of **A** for DASA **1** (sample **1**) in dichloromethane.

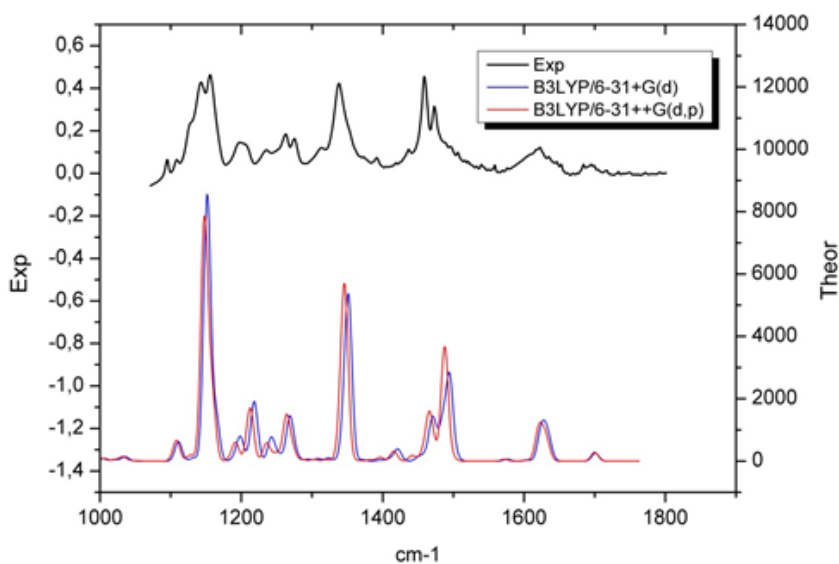


Figure S6.5 | A comparison between experimental and scaled theoretical ground state IR spectra of **A** for DASA **2** (sample **2**) in chloroform.

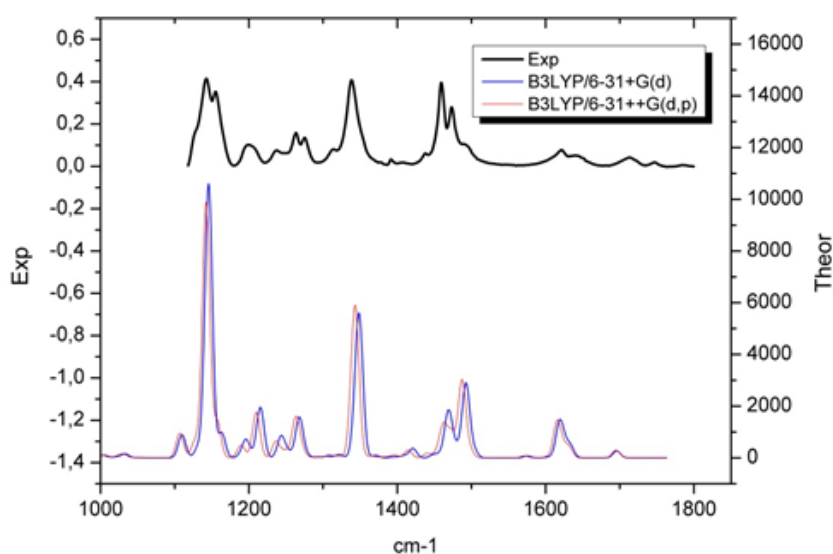


Figure S6.6 | A comparison between experimental and scaled theoretical ground state IR spectra of **A** for DASA **2** (sample **2**) in dichloromethane.

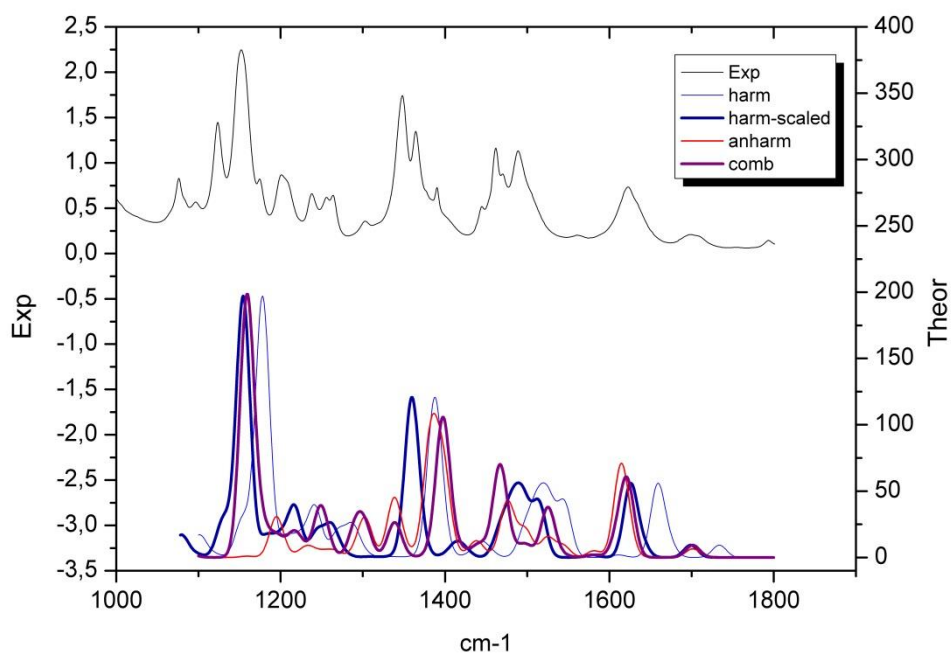


Figure S6.7 | A comparison between experimental and simulated ground state IR spectra of **A** for DASA **1** (sample **1**) in chloroform. The notation harm, harm-scaled, **anharm** and **comb** stands for the harmonic frequencies/harmonic intensities, scaled harmonic frequencies (using scaling factor 0.98)/harmonic intensities, **anharmonic frequencies/anharmonic intensities** and **anharmonic frequencies/anharmonic intensities** models.

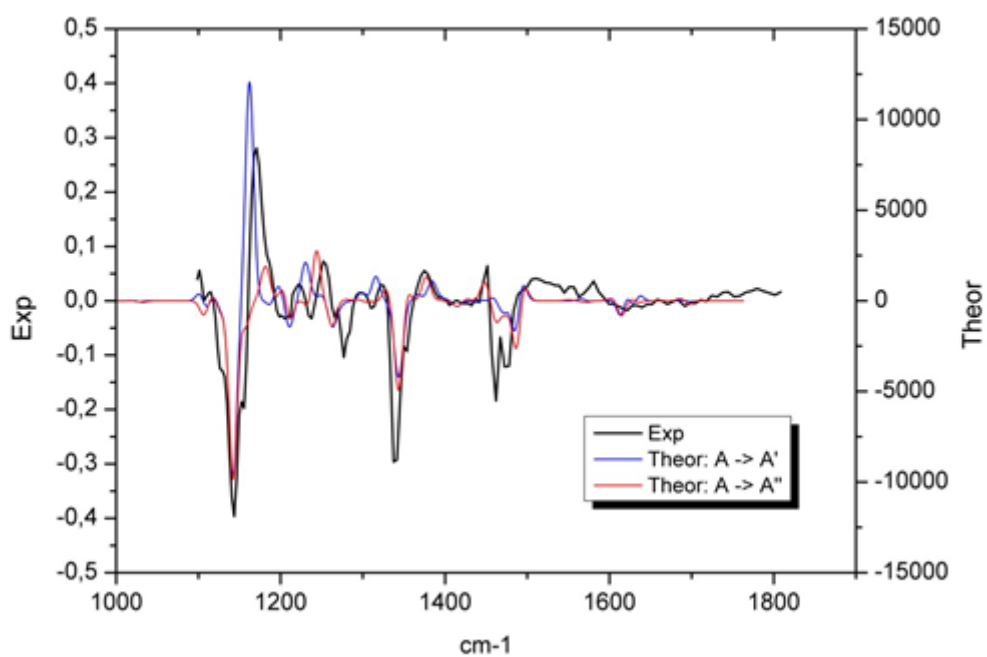


Figure S6.8 | A comparison between experimental and simulated (scaled) long-lasting component of IR EADS ($GS(A') - GS(A)$) of DASA 2 (sample 2) in DCM. The blue and red lines correspond to a conversion of **A** to **A'** and **A** to **A''**, respectively.

6.3 Vertical excitation energies and electronic density differences (EDD)

Vertical excitation energies were computed using TD-DFT for **A** form of compound **1** and **2** in dichloromethane (DCM) and in chloroform (CHCl₃) using M06-2X and the SMD solvent model. Structures were optimized with the 6-31+G(d) basis while excitation energies with a larger basis set, namely 6-311++G(2df,2p). To compute the solvation response of the chromophore excitation, the Linear Response (LR) and the corrected LR were employed in the non-equilibrium limit.

Table S6.2 | Maximum absorption wavelength in nm (vertical excitation energies in eV are in parentheses) for **A** form of DASA **1** and **2** in dichloromethane (DCM) and in chloroform (CHCl₃) evaluated at the SMD/M06-2X/6-311++G(2df,2p)//SMD/M06-2X/6-31+G(d) level of theory.

System	Solvent	LR(neq)	cLR(neq)
DASA 1	DCM	461 (2.69)	426 (2.91)
	CHCl ₃	466 (2.66)	428 (2.90)
DASA 2	DCM	508 (2.44)	466(2.66)
	CHCl ₃	511 (2.43)	466 (2.66)

The charge-transfer (CT) charge (q_{CT}) and distance (d_{CT}) for both DASA generations (**A** species) were quantified through a well-established analysis considering the difference of total densities between the excited and the ground states (EDD).²¹ Figure S6.9 presents the EDD plots using a threshold of 0.001 a.u.. A delocalized π - π^* state is observed which is depicted by an alternation of loss (blue) and gain (red) in the EDD plots. The modification of the functional group induces a negligible change in q_{CT} (0.34 e vs 0.38 e for **1** and **2**, respectively) while the d_{CT} is twice larger in **2** (1.22 Å) than in **1** (0.58 Å). The CT distances are relatively small compared to classical push-pull dyes in which d_{CT} attains *ca.* 5 Å.

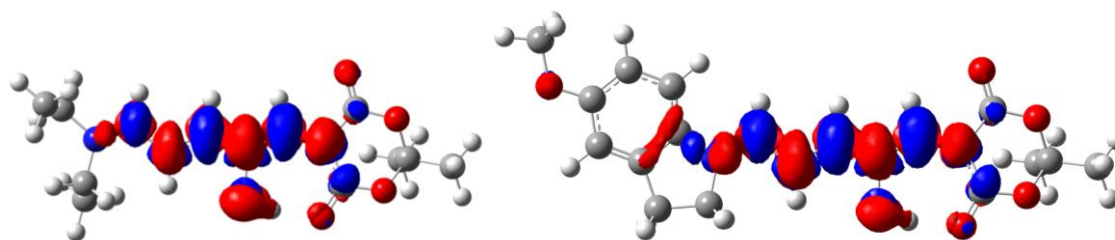


Figure S6.9 | Electronic density difference plots between the ES and the GS of **A** for DASA **1** (left) and **2** (right) obtained in chloroform at the M06-2X/6-311++G(2df,2p) level of theory. The blue (red) regions correspond to decrease (increase) in electron density upon electronic transition. A contour threshold of 0.001 a.u. has been applied.

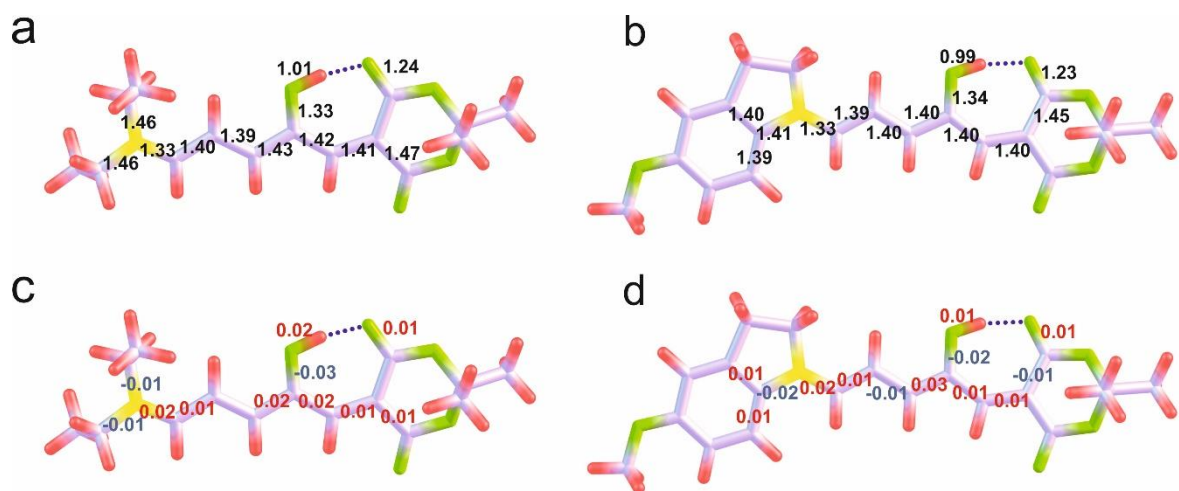


Figure S6.10 | Optimized ES geometries of the **A** form of DASA **1** (a) and **2** (b), and geometry difference plots between the ES and the GS of **A** for DASA **1** (c) and **2** (d) obtained in chloroform at the SMD/M06-2X/6-31+G(d) level of theory. The red/blue values correspond to the increase/decrease of the bond lengths (in Å) with respect to the ground state structure.

6.4 Cartesian coordinates of various forms of compounds **1** and **2**

Below we report the Cartesian coordinates of all relevant structures (**A**, **A***, **A'**, **A''**, **TS** and **B**) of **1** and **2** in chloroform optimized at the SMD/M06-2X/6-31+G(d) level of theory.

Structure 1-A

C	-4.962515000	-0.134639000	0.207077000
C	-2.849880000	-0.881304000	-0.635140000
C	-2.295945000	0.366301000	-0.168681000
C	-3.204251000	1.484223000	0.069941000
C	-6.386960000	-0.211342000	-0.291391000
C	-4.819044000	-0.546838000	1.664106000
C	-0.923899000	0.653879000	-0.045064000
C	0.229170000	-0.120894000	-0.143503000
C	1.463492000	0.515476000	0.052604000
C	2.695894000	-0.127237000	-0.018971000
C	3.861825000	0.612096000	0.188289000
C	5.416418000	-1.241383000	-0.129096000
C	5.309762000	-2.088011000	1.134572000
C	6.237811000	1.070540000	0.365967000
C	6.855090000	1.544805000	-0.943853000
N	5.105428000	0.166238000	0.139763000
O	-2.220650000	-1.831026000	-1.102128000
O	-2.871632000	2.638963000	0.261329000
O	-4.538825000	1.211415000	0.021768000
O	-4.196937000	-1.005220000	-0.629859000
O	0.272894000	-1.459809000	-0.380785000
H	-7.020091000	0.451961000	0.303554000
H	-6.755655000	-1.236116000	-0.198537000
H	-6.428440000	0.094197000	-1.340016000
H	-3.779473000	-0.484113000	1.998689000
H	-5.166058000	-1.576330000	1.786735000
H	-5.429165000	0.111851000	2.288038000
H	-0.728450000	1.696789000	0.192917000
H	1.438385000	1.578891000	0.281020000
H	2.728837000	-1.189942000	-0.233420000
H	3.766708000	1.674123000	0.415443000
H	6.433151000	-1.275106000	-0.529162000
H	4.745871000	-1.606570000	-0.911827000
H	6.007727000	-1.731669000	1.898997000
H	5.553640000	-3.129764000	0.905621000
H	4.296872000	-2.054249000	1.547093000
H	6.973053000	0.532237000	0.972949000
H	5.879912000	1.918873000	0.954565000
H	7.195738000	0.701362000	-1.552921000
H	7.717904000	2.185544000	-0.737296000
H	6.127184000	2.119561000	-1.525122000
H	-0.616268000	-1.753808000	-0.699413000

Structure 1-A*

C	-4.981526000	-0.205129000	0.178674000
C	-2.811828000	-0.886896000	-0.552990000
C	-2.314347000	0.406264000	-0.154640000
C	-3.291555000	1.484421000	0.023916000
C	-6.383237000	-0.367931000	-0.360132000
C	-4.867389000	-0.547965000	1.656308000
C	-0.957052000	0.771458000	-0.004272000
C	0.249963000	0.039430000	-0.123951000
C	1.501608000	0.668314000	0.141403000
C	2.724491000	0.011527000	0.014274000
C	3.941521000	0.663012000	0.263921000
C	5.365568000	-1.278153000	-0.199661000
C	5.168556000	-2.218849000	0.987966000
C	6.347344000	0.939382000	0.404116000
C	6.919332000	1.492241000	-0.898816000
N	5.160085000	0.119785000	0.171571000
O	-2.118176000	-1.847199000	-0.917480000
O	-3.010326000	2.657867000	0.179691000
O	-4.609514000	1.148713000	-0.051982000
O	-4.149231000	-1.072768000	-0.594854000
O	0.315585000	-1.244684000	-0.479552000
H	-7.064359000	0.289522000	0.186117000
H	-6.707869000	-1.404004000	-0.234221000
H	-6.404528000	-0.108621000	-1.421705000
H	-3.841412000	-0.428777000	2.018023000
H	-5.177140000	-1.584377000	1.814759000
H	-5.520960000	0.113035000	2.231879000
H	-0.812617000	1.813259000	0.267702000
H	1.478083000	1.713026000	0.441971000
H	2.719507000	-1.032825000	-0.285152000
H	3.927003000	1.709605000	0.564419000
H	6.386059000	-1.362549000	-0.583958000
H	4.687090000	-1.532844000	-1.020657000
H	5.874735000	-1.980161000	1.789852000
H	5.339116000	-3.253610000	0.674353000
H	4.152554000	-2.141866000	1.386855000
H	7.087852000	0.317303000	0.918913000
H	6.070739000	1.755042000	1.077709000
H	7.186474000	0.684336000	-1.587661000
H	7.820930000	2.077912000	-0.691973000
H	6.188480000	2.140895000	-1.392105000
H	-0.605742000	-1.584979000	-0.699386000

Structure 1-A'

C	4.564182000	-0.594808000	0.368242000
C	3.032369000	1.063197000	-0.430504000
C	1.979930000	0.098235000	-0.211245000
C	2.341305000	-1.316031000	-0.146144000
C	5.952103000	-1.032482000	-0.037261000
C	4.422438000	-0.380332000	1.867100000
C	0.602262000	0.378151000	-0.189088000
C	-0.135187000	1.557312000	-0.176884000
C	-1.541404000	1.531129000	-0.156837000
C	-2.413684000	0.446216000	-0.084194000
C	-3.785111000	0.697348000	-0.074559000
C	-4.489711000	-1.633979000	0.091192000
C	-4.231654000	-2.239332000	-1.284512000
C	-6.162586000	0.228112000	0.019361000
C	-6.717393000	0.309554000	1.436050000
N	-4.758697000	-0.195728000	0.006544000
O	2.886645000	2.237237000	-0.767726000
O	1.560956000	-2.248956000	-0.189752000
O	3.670289000	-1.607722000	-0.081232000
O	4.308033000	0.624123000	-0.333504000
O	0.400622000	2.815159000	-0.140836000
H	6.199008000	-1.975356000	0.457253000
H	6.678610000	-0.271576000	0.258925000
H	5.994355000	-1.170946000	-1.120613000
H	3.411263000	-0.059684000	2.133653000
H	5.131328000	0.385401000	2.193375000
H	4.642309000	-1.315796000	2.388547000
H	-0.000605000	-0.524949000	-0.163024000
H	-1.998168000	2.521896000	-0.188217000
H	-2.046001000	-0.573577000	-0.040598000
H	-4.120361000	1.731860000	-0.141341000
H	-5.363927000	-2.097801000	0.555844000
H	-3.642178000	-1.795001000	0.763631000
H	-5.096954000	-2.093113000	-1.939021000
H	-4.048690000	-3.314015000	-1.190740000
H	-3.358492000	-1.782704000	-1.760320000
H	-6.728515000	-0.490687000	-0.582280000
H	-6.226977000	1.199225000	-0.478017000
H	-6.629374000	-0.650876000	1.953874000
H	-7.776258000	0.584860000	1.406219000
H	-6.178805000	1.065703000	2.016069000
H	1.349804000	2.764765000	-0.408921000

Structure 1-A''

C	-3.698568000	-0.995813000	-0.172750000
C	-2.606212000	1.132559000	-0.277603000
C	-1.480760000	0.521811000	0.381596000
C	-1.683042000	-0.735778000	1.087451000
C	-5.106966000	-1.449187000	0.133606000
C	-3.124270000	-1.640381000	-1.425511000
C	-0.169442000	1.049273000	0.438829000
C	0.384024000	2.279113000	0.093072000
C	1.767178000	2.511784000	0.277215000
C	2.787701000	1.570792000	0.266277000
C	2.643954000	0.320027000	-0.360180000
C	4.653495000	-0.679428000	0.596900000
C	5.876493000	-0.090336000	-0.098251000
C	3.273648000	-1.900730000	-1.096570000
C	2.530498000	-2.974392000	-0.312062000
N	3.485308000	-0.692637000	-0.287963000
O	-2.644523000	2.260856000	-0.770096000
O	-0.868637000	-1.282584000	1.810172000
O	-2.908308000	-1.323304000	0.963315000
O	-3.758326000	0.422899000	-0.334381000
O	-0.324090000	3.377199000	-0.289197000
H	-5.118361000	-2.530858000	0.289816000
H	-5.765485000	-1.200540000	-0.702535000
H	-5.466623000	-0.950266000	1.037283000
H	-2.107843000	-1.287493000	-1.625066000
H	-3.755189000	-1.396209000	-2.284461000
H	-3.101434000	-2.725817000	-1.295919000
H	0.527985000	0.377128000	0.930890000
H	2.042214000	3.554825000	0.435011000
H	3.757437000	1.857130000	0.662252000
H	1.793979000	0.167719000	-1.023718000
H	4.844044000	-1.714075000	0.895675000
H	4.395942000	-0.117829000	1.498626000
H	6.140979000	-0.675976000	-0.984475000
H	6.731086000	-0.099353000	0.584927000
H	5.693410000	0.942369000	-0.410689000
H	4.257983000	-2.256461000	-1.417031000
H	2.716080000	-1.616256000	-1.992183000
H	3.076528000	-3.257632000	0.593313000
H	2.410112000	-3.868940000	-0.930795000
H	1.537480000	-2.619655000	-0.018461000
H	-1.262786000	3.110251000	-0.457334000

Structure 1-TS

C	3.913959000	-1.007754000	0.075437000
C	2.848843000	1.133173000	-0.121657000
C	1.592079000	0.390556000	-0.340097000
C	1.703914000	-1.005455000	-0.848260000
C	5.248201000	-1.552357000	-0.372021000
C	3.583278000	-1.326669000	1.522460000
C	0.326004000	0.871077000	-0.195210000
C	-0.222403000	2.123794000	0.284711000
C	-1.570597000	2.288000000	0.292100000
C	-2.577669000	1.307161000	-0.169582000
C	-3.202072000	0.471316000	0.688406000
C	-4.554519000	-0.670571000	-0.986490000
C	-5.542330000	0.369371000	-1.508163000
C	-4.322910000	-1.572228000	1.322376000
C	-3.260711000	-2.648285000	1.110867000
N	-4.191121000	-0.440390000	0.406914000
O	2.943426000	2.343984000	-0.022067000
O	0.792688000	-1.632884000	-1.331672000
O	2.933514000	-1.562275000	-0.800970000
O	3.978469000	0.414849000	-0.114766000
O	0.547686000	3.123966000	0.782330000
H	5.249789000	-2.640198000	-0.269660000
H	6.042333000	-1.132517000	0.250018000
H	5.426782000	-1.286351000	-1.416866000
H	2.610919000	-0.918812000	1.816063000
H	4.352497000	-0.901153000	2.172149000
H	3.562311000	-2.411386000	1.655307000
H	-0.451320000	0.163713000	-0.477240000
H	-1.913094000	3.258022000	0.659219000
H	-2.835106000	1.323536000	-1.227067000
H	-2.924613000	0.497824000	1.742926000
H	-5.007148000	-1.664556000	-1.051740000
H	-3.648309000	-0.692879000	-1.611595000
H	-6.482894000	0.311232000	-0.950852000
H	-5.756836000	0.192089000	-2.567492000
H	-5.150154000	1.385395000	-1.404777000
H	-5.325595000	-1.992995000	1.192633000
H	-4.267606000	-1.183535000	2.344955000
H	-3.310495000	-3.060212000	0.096890000
H	-3.400056000	-3.472424000	1.819011000
H	-2.256836000	-2.233745000	1.259347000
H	1.478624000	3.013781000	0.488265000

Structure 1-B

C	4.452450000	-1.279850000	0.449691000
H	4.053975000	-2.102909000	1.049229000
H	5.134976000	-0.686123000	1.063651000
H	5.002054000	-1.689324000	-0.402185000
C	3.316321000	-0.409744000	-0.041950000
C	3.802044000	0.756123000	-0.893972000
H	4.328886000	0.369643000	-1.771027000
H	4.489960000	1.372493000	-0.308260000
H	2.969593000	1.380883000	-1.228429000
C	1.186165000	-0.805848000	-1.069740000
C	0.689416000	0.211671000	-0.225733000
C	1.391294000	0.600499000	0.939270000
C	-0.678291000	0.773535000	-0.423828000
H	-1.060579000	0.434244000	-1.397442000
C	-0.736090000	2.309596000	-0.478229000
C	-1.966236000	2.749973000	0.228679000
H	-2.297323000	3.782332000	0.253267000
C	-2.541584000	1.701311000	0.824832000
H	-3.450666000	1.725372000	1.421933000
C	-1.717262000	0.450379000	0.667593000
C	-1.757346000	-2.038324000	0.316837000
H	-1.061680000	-1.925227000	-0.519130000
H	-2.473006000	-2.826055000	0.070556000
C	-1.046092000	-2.344527000	1.620862000
H	-0.218984000	-1.657555000	1.818136000
H	-0.625843000	-3.351622000	1.546686000
H	-1.736906000	-2.333265000	2.471584000
C	-3.421613000	-0.625061000	-0.866436000
H	-3.577605000	0.441769000	-1.039937000
H	-2.841642000	-1.031639000	-1.697407000
C	-4.748549000	-1.341542000	-0.693283000
H	-4.620200000	-2.408897000	-0.489624000
H	-5.324224000	-1.245195000	-1.617615000
H	-5.334286000	-0.893485000	0.116485000
H	-1.212904000	0.237905000	1.614673000
H	-3.206964000	-0.854431000	1.171024000
N	-2.566341000	-0.762622000	0.370920000
O	2.646028000	0.070674000	1.122013000
O	2.458715000	-1.259695000	-0.799576000
O	0.949258000	1.329536000	1.830821000
O	0.581875000	-1.372571000	-1.985680000
O	0.074123000	3.025844000	-1.023848000

Structure 2-A

C	-6.836613000	0.285349000	0.303672000
C	-4.866657000	-0.873233000	-0.409139000
C	-4.150966000	0.371737000	-0.229668000
C	-4.918904000	1.618365000	-0.218362000
C	-8.282744000	0.276049000	-0.131948000
C	-6.665870000	0.175578000	1.810551000
C	-2.758584000	0.513207000	-0.184981000
C	-1.696621000	-0.398393000	-0.147626000
C	-0.399727000	0.115798000	-0.101479000
C	0.754455000	-0.674722000	-0.068048000
C	2.001481000	-0.069523000	-0.028117000
O	-4.370039000	-1.965039000	-0.678330000
O	-4.448079000	2.736715000	-0.288294000
O	-6.274277000	1.501352000	-0.178018000
O	-6.214753000	-0.827817000	-0.345891000
O	-1.816132000	-1.751925000	-0.120813000
H	-8.805664000	1.124832000	0.315936000
H	-8.759764000	-0.651431000	0.194654000
H	-8.341281000	0.349192000	-1.220855000
H	-5.609902000	0.184804000	2.096708000
H	-7.116984000	-0.756497000	2.161053000
H	-7.167170000	1.018661000	2.293516000
H	-2.438750000	1.552233000	-0.159120000
H	-0.292976000	1.198315000	-0.086052000
H	0.657045000	-1.755430000	-0.081076000
H	2.066147000	1.016662000	-0.029510000
H	-2.746136000	-1.995902000	-0.350823000
C	4.449009000	-0.130457000	0.017036000
C	3.266692000	-2.187673000	0.042482000
C	5.421801000	-1.128147000	0.132479000
C	4.795622000	1.209172000	-0.080540000
C	4.768869000	-2.484995000	0.229332000
H	2.653336000	-2.572040000	0.861566000
C	6.761632000	-0.793807000	0.156227000
C	6.151962000	1.551306000	-0.055586000
H	4.051116000	1.993207000	-0.178627000
H	4.963776000	-2.942606000	1.203937000
C	7.130232000	0.558160000	0.062477000
H	7.537275000	-1.549666000	0.244917000
H	6.426592000	2.596925000	-0.132309000
N	3.162166000	-0.714796000	0.015059000
O	8.465877000	0.803911000	0.092231000
C	8.898517000	2.150368000	-0.017597000
H	8.524105000	2.754449000	0.816844000
H	9.987811000	2.117775000	0.017594000
H	8.577677000	2.590553000	-0.968729000
H	2.877019000	-2.583672000	-0.900656000
H	5.139262000	-3.169200000	-0.538450000

Structure 2-A*

C	-6.885519000	0.153971000	0.332211000
C	-4.838842000	-0.889107000	-0.328175000
C	-4.202736000	0.401920000	-0.237810000
C	-5.061860000	1.588301000	-0.259268000
C	-8.327948000	0.025711000	-0.097486000
C	-6.707855000	0.121329000	1.842525000
C	-2.811875000	0.647916000	-0.226231000
C	-1.687693000	-0.207778000	-0.209201000
C	-0.379443000	0.345769000	-0.158600000
C	0.774011000	-0.435738000	-0.125757000
C	2.054318000	0.122785000	-0.096647000
O	-4.263129000	-1.969625000	-0.510900000
O	-4.666280000	2.733193000	-0.376186000
O	-6.407447000	1.382687000	-0.202293000
O	-6.187571000	-0.939053000	-0.269722000
O	-1.755201000	-1.543503000	-0.225266000
H	-8.909660000	0.850992000	0.320926000
H	-8.737162000	-0.920925000	0.264539000
H	-8.393051000	0.054150000	-1.188131000
H	-5.653503000	0.203780000	2.124026000
H	-7.103658000	-0.818969000	2.235572000
H	-7.256392000	0.954853000	2.289216000
H	-2.556795000	1.703957000	-0.212300000
H	-0.297807000	1.429476000	-0.147968000
H	0.660224000	-1.516700000	-0.123887000
H	2.178840000	1.201268000	-0.121180000
H	-2.707259000	-1.831429000	-0.353339000
C	4.481923000	-0.099798000	0.000588000
C	3.195486000	-2.076394000	0.047075000
C	5.410572000	-1.152488000	0.094640000
C	4.903247000	1.230604000	-0.042521000
C	4.684012000	-2.472880000	0.112154000
H	2.637424000	-2.381356000	0.938481000
C	6.760868000	-0.888622000	0.146924000
C	6.272256000	1.496994000	0.008794000
H	4.201099000	2.054770000	-0.115435000
H	4.906845000	-3.039969000	1.020436000
C	7.198806000	0.449361000	0.103029000
H	7.497538000	-1.684293000	0.218199000
H	6.603579000	2.528530000	-0.024904000
N	3.186901000	-0.602391000	-0.032862000
O	8.540986000	0.624756000	0.155860000
C	9.048366000	1.948552000	0.080969000
H	8.700090000	2.552240000	0.926638000
H	10.133434000	1.854565000	0.123731000
H	8.759298000	2.426023000	-0.862148000
H	2.688569000	-2.482772000	-0.833733000
H	4.968615000	-3.091540000	-0.743920000

Structure 2-A'

C	6.455817000	-0.621630000	0.224281000
C	4.911606000	1.110042000	-0.368480000
C	3.859084000	0.124707000	-0.218393000
C	4.221634000	-1.293036000	-0.307520000
C	7.832881000	-1.016198000	-0.254357000
C	6.345736000	-0.558389000	1.739288000
C	2.491063000	0.397746000	-0.128863000
C	1.753771000	1.574588000	0.041287000
C	0.356527000	1.544051000	0.090395000
C	-0.518945000	0.450695000	0.017120000
C	-1.882950000	0.677270000	0.086989000
O	4.755654000	2.308344000	-0.587367000
O	3.437221000	-2.213626000	-0.427040000
O	5.549608000	-1.585307000	-0.304636000
O	6.185001000	0.662001000	-0.347003000
O	2.304062000	2.811381000	0.224745000
H	8.085834000	-2.005915000	0.134128000
H	8.568456000	-0.291746000	0.104162000
H	7.851923000	-1.040825000	-1.346909000
H	5.340408000	-0.267857000	2.058301000
H	7.061534000	0.171678000	2.126288000
H	6.576502000	-1.541321000	2.158447000
H	1.885498000	-0.501960000	-0.185510000
H	-0.103738000	2.525693000	0.213302000
H	-0.149519000	-0.562627000	-0.102805000
H	-2.249155000	1.696336000	0.192883000
H	3.237914000	2.797874000	-0.093247000
C	-4.216967000	-0.057911000	0.035580000
C	-2.517718000	-1.704422000	-0.112254000
C	-4.879832000	-1.289109000	0.012878000
C	-4.916831000	1.139382000	0.050026000
C	-3.878386000	-2.417941000	0.024844000
H	-2.059457000	-1.868816000	-1.093404000
C	-6.259947000	-1.335971000	0.005304000
C	-6.315564000	1.095481000	0.044005000
H	-4.413643000	2.101025000	0.059003000
H	-4.045085000	-3.123939000	-0.792381000
C	-6.984524000	-0.132711000	0.020543000
H	-6.799434000	-2.279088000	-0.012252000
H	-6.866283000	2.029152000	0.052970000
N	-2.819975000	-0.266607000	0.031903000
O	-8.336923000	-0.264040000	0.008329000
C	-9.119968000	0.918242000	0.013736000
H	-8.918445000	1.529182000	-0.873679000
H	-10.159170000	0.589113000	-0.001500000
H	-8.938414000	1.507853000	0.919672000
H	-1.803708000	-2.001089000	0.659940000
H	-3.938106000	-2.975818000	0.964600000

Structure 2-A''

C	3.797943000	2.271136000	0.245194000
C	4.001464000	-0.009688000	-0.458598000
C	2.800061000	-0.285716000	0.300016000
C	2.391315000	0.669361000	1.329679000
C	4.777709000	3.325196000	0.703614000
C	2.826504000	2.778687000	-0.809074000
C	1.978281000	-1.414936000	0.164583000
C	2.072010000	-2.602267000	-0.575662000
C	1.032736000	-3.544172000	-0.532801000
C	-0.313322000	-3.330449000	-0.210379000
C	-0.934569000	-2.089700000	-0.319825000
O	4.578733000	-0.785836000	-1.216312000
O	1.506308000	0.490414000	2.144256000
O	3.096394000	1.832594000	1.402752000
O	4.581076000	1.197955000	-0.285767000
O	3.176493000	-3.001708000	-1.262604000
H	4.233641000	4.167031000	1.139223000
H	5.363100000	3.679278000	-0.148692000
H	5.450819000	2.903077000	1.454218000
H	2.135067000	1.992880000	-1.128495000
H	3.385555000	3.128495000	-1.680962000
H	2.248317000	3.610222000	-0.397405000
H	1.119437000	-1.384480000	0.828881000
H	1.322928000	-4.559155000	-0.803980000
H	-0.916530000	-4.197401000	0.045194000
H	-0.421390000	-1.272173000	-0.820475000
H	3.836739000	-2.265724000	-1.273600000
C	-2.885880000	-0.628432000	-0.137305000
C	-2.998274000	-2.774469000	0.859037000
C	-4.098118000	-0.662863000	0.558675000
C	-2.525251000	0.464110000	-0.911932000
C	-4.216543000	-1.954903000	1.329986000
H	-3.288820000	-3.597696000	0.197500000
C	-4.966354000	0.408976000	0.495140000
C	-3.401397000	1.552897000	-0.975860000
H	-1.595020000	0.494121000	-1.471060000
H	-5.154743000	-2.475034000	1.121275000
C	-4.612971000	1.528147000	-0.276870000
H	-5.912707000	0.410217000	1.028903000
H	-3.126351000	2.409525000	-1.579881000
N	-2.168722000	-1.823706000	0.093175000
O	-5.517472000	2.541352000	-0.287762000
C	-5.203221000	3.704827000	-1.035739000
H	-5.104171000	3.473087000	-2.102419000
H	-6.039896000	4.388325000	-0.889758000
H	-4.282687000	4.173161000	-0.668985000
H	-2.406147000	-3.178950000	1.683537000
H	-4.171081000	-1.765477000	2.407000000

Structure 2-TS

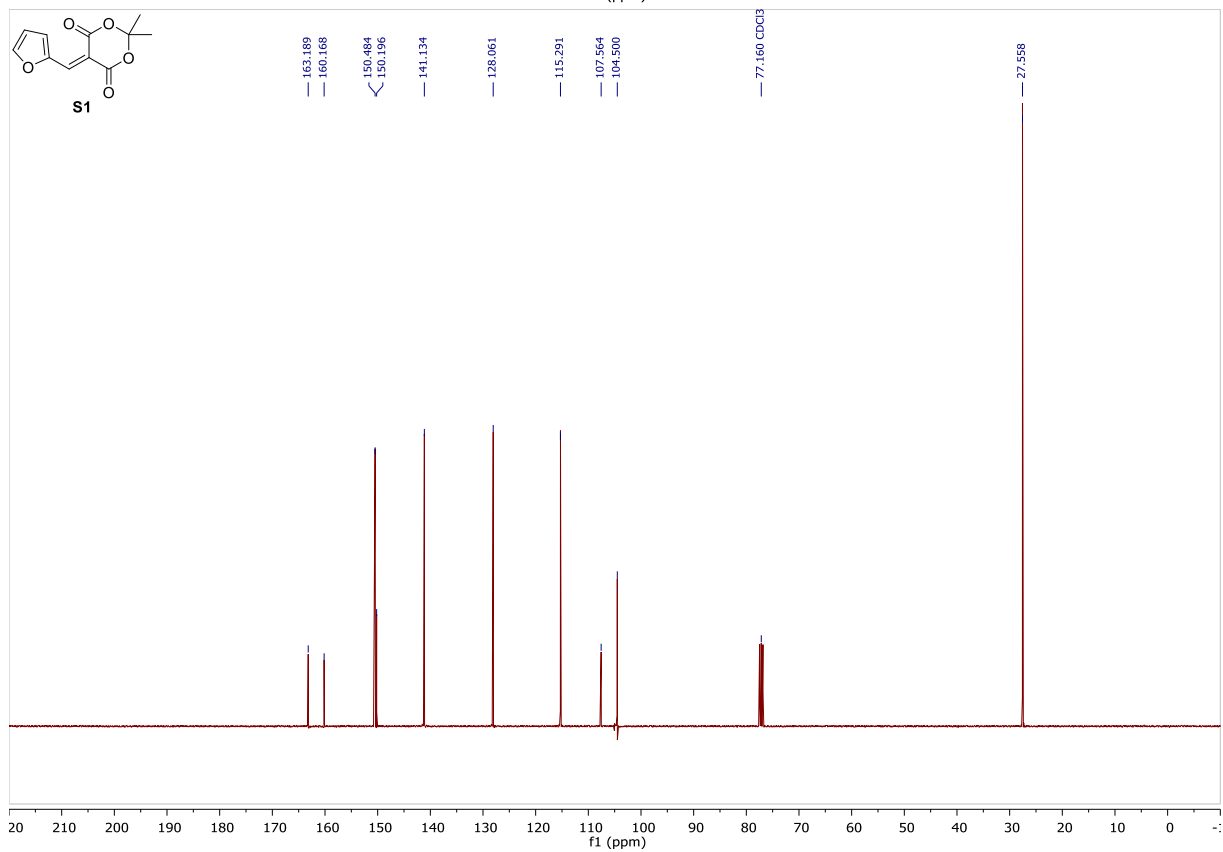
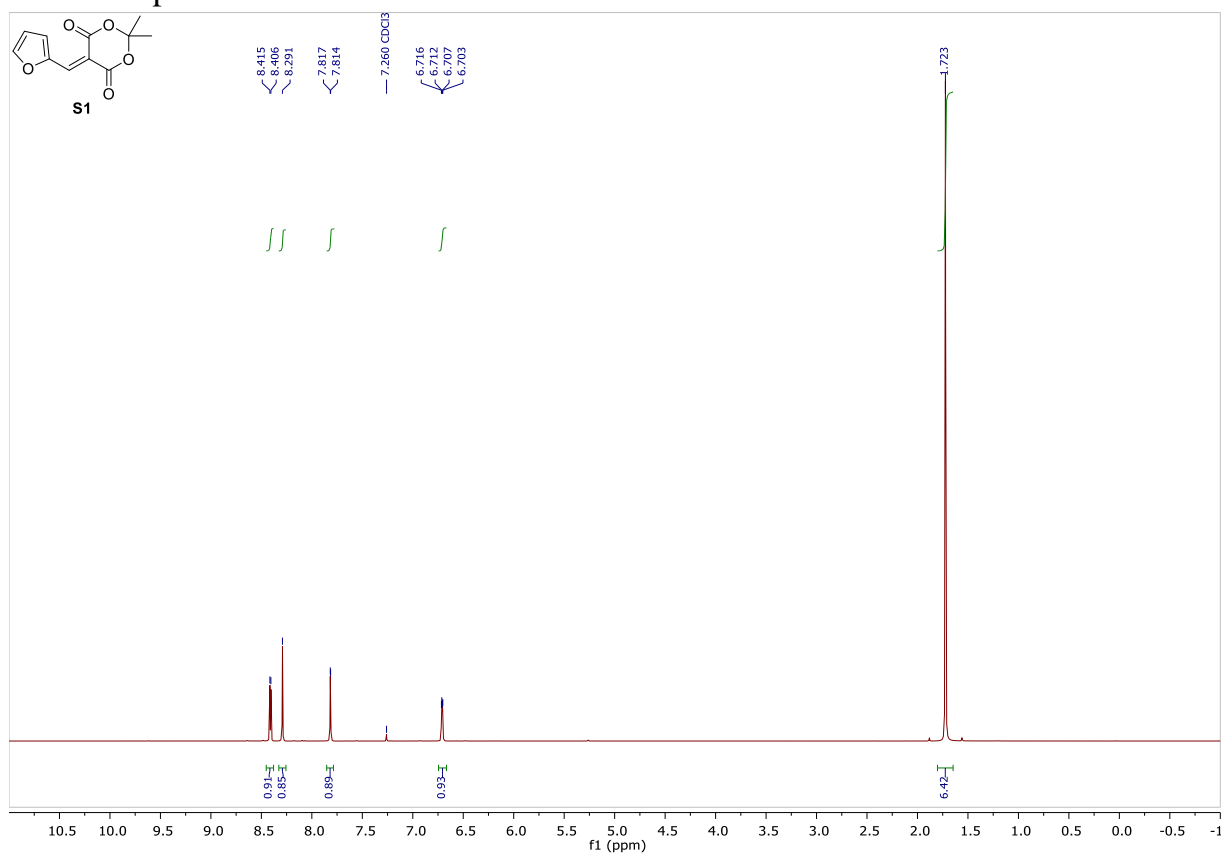
C	4.740139000	2.001140000	0.178009000
C	4.556002000	-0.328411000	-0.363419000
C	3.201240000	-0.264817000	0.220949000
C	2.940971000	0.812653000	1.217957000
C	5.869993000	2.867780000	0.677126000
C	3.993101000	2.597015000	-1.001537000
C	2.177667000	-1.135029000	0.004088000
C	2.002580000	-2.277497000	-0.872829000
C	0.820651000	-2.944576000	-0.854358000
C	-0.352628000	-2.638014000	-0.006822000
C	-1.387038000	-1.898592000	-0.457628000
O	5.039371000	-1.300846000	-0.916079000
O	2.006835000	0.825740000	1.982034000
O	3.860199000	1.800030000	1.283401000
O	5.334055000	0.746717000	-0.195240000
O	2.950393000	-2.682576000	-1.753521000
H	5.473200000	3.833521000	0.999422000
H	6.591740000	3.027085000	-0.127711000
H	6.367445000	2.381073000	1.519758000
H	3.180725000	1.945721000	-1.338957000
H	4.687993000	2.749940000	-1.831175000
H	3.569344000	3.560560000	-0.707208000
H	1.286905000	-0.925301000	0.592709000
H	0.763411000	-3.800815000	-1.529376000
H	-0.382029000	-3.083153000	0.986653000
H	-1.351921000	-1.468944000	-1.456600000
H	3.825077000	-2.305757000	-1.511051000
C	-3.456205000	-0.618872000	-0.078617000
C	-2.719035000	-2.052747000	1.628854000
C	-4.410146000	-0.507805000	0.945611000
C	-3.511720000	0.210062000	-1.189332000
C	-4.129355000	-1.553259000	2.000003000
H	-2.615866000	-3.138401000	1.710257000
C	-5.427105000	0.420849000	0.861590000
C	-4.546977000	1.155019000	-1.277737000
H	-2.777480000	0.151355000	-1.987080000
H	-4.861865000	-2.365835000	1.929815000
C	-5.494748000	1.264920000	-0.261005000
H	-6.174893000	0.520797000	1.644243000
H	-4.584709000	1.802535000	-2.146365000
N	-2.536794000	-1.632510000	0.236617000
O	-6.524173000	2.162257000	-0.260780000
C	-6.615902000	3.055004000	-1.355445000
H	-6.767621000	2.514298000	-2.297447000
H	-7.482947000	3.686241000	-1.157236000
H	-5.719224000	3.682092000	-1.431452000
H	-1.944928000	-1.583382000	2.254232000
H	-4.167159000	-1.155578000	3.016983000

Structure 2-B

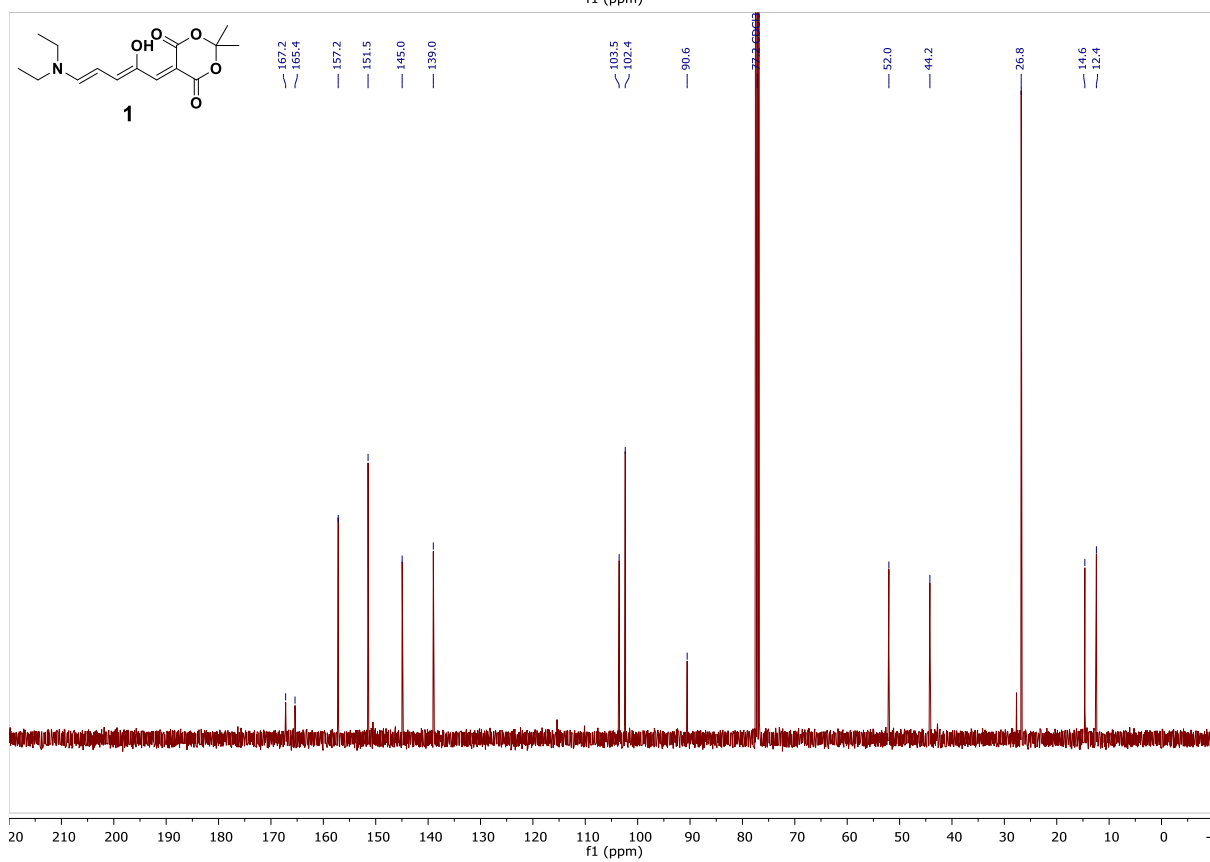
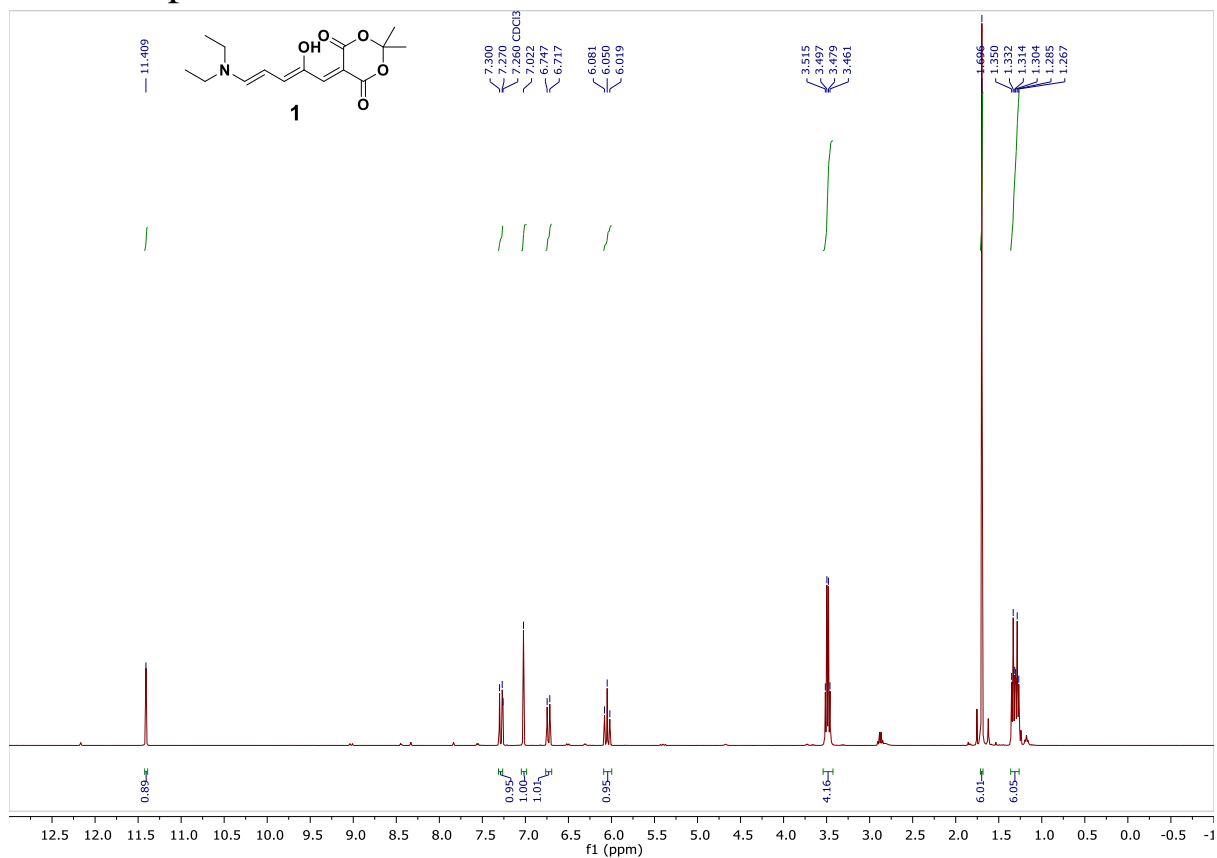
C	0.662292000	-2.711699000	0.809044000
C	-0.623851000	-1.810088000	-1.089852000
C	-1.598554000	-1.159741000	-0.115174000
C	-1.113269000	-1.156778000	1.324716000
C	0.861462000	-4.173723000	1.132867000
C	1.893507000	-1.856545000	1.030326000
C	-2.278350000	0.100054000	-0.533855000
C	-3.701288000	0.066913000	-0.880440000
C	-4.218487000	1.488773000	-0.831475000
C	-3.220031000	2.261604000	-0.404117000
C	-1.992267000	1.409281000	-0.220989000
O	-0.722974000	-1.705646000	-2.284813000
O	-1.463028000	-0.373520000	2.166118000
O	-0.374350000	-2.236935000	1.669137000
O	0.292668000	-2.650221000	-0.578525000
H	1.142096000	-4.280990000	2.183646000
H	1.658727000	-4.581804000	0.506395000
H	-0.063132000	-4.726220000	0.946237000
H	1.654032000	-0.802442000	0.863976000
H	2.688270000	-2.157196000	0.342638000
H	2.238927000	-1.980693000	2.060200000
H	-5.226264000	1.770124000	-1.111179000
H	-3.218933000	3.336247000	-0.259270000
C	0.469098000	1.524794000	-0.104604000
C	-0.742983000	3.132045000	1.092904000
C	1.366157000	2.071015000	0.824615000
C	0.913105000	0.824289000	-1.215526000
C	0.584944000	2.878250000	1.835670000
H	-0.689420000	4.057821000	0.507677000
C	2.722978000	1.863287000	0.680054000
C	2.290148000	0.615468000	-1.367727000
H	0.221304000	0.478685000	-1.976352000
H	1.080468000	3.809648000	2.117443000
C	3.186716000	1.117756000	-0.421003000
H	3.443975000	2.275202000	1.381036000
H	2.641451000	0.065185000	-2.233290000
N	-0.838373000	1.972311000	0.178070000
O	4.534426000	0.950489000	-0.484103000
C	5.066935000	0.278912000	-1.614630000
H	4.820385000	0.811182000	-2.540557000
H	6.148243000	0.271548000	-1.475379000
H	4.700136000	-0.752514000	-1.672068000
H	-1.607500000	3.160175000	1.756283000
H	0.408658000	2.288644000	2.743334000
O	-4.383821000	-0.923128000	-1.098091000
H	-2.405761000	-1.920294000	-0.089866000

7 ^1H - and ^{13}C -NMR Spectra

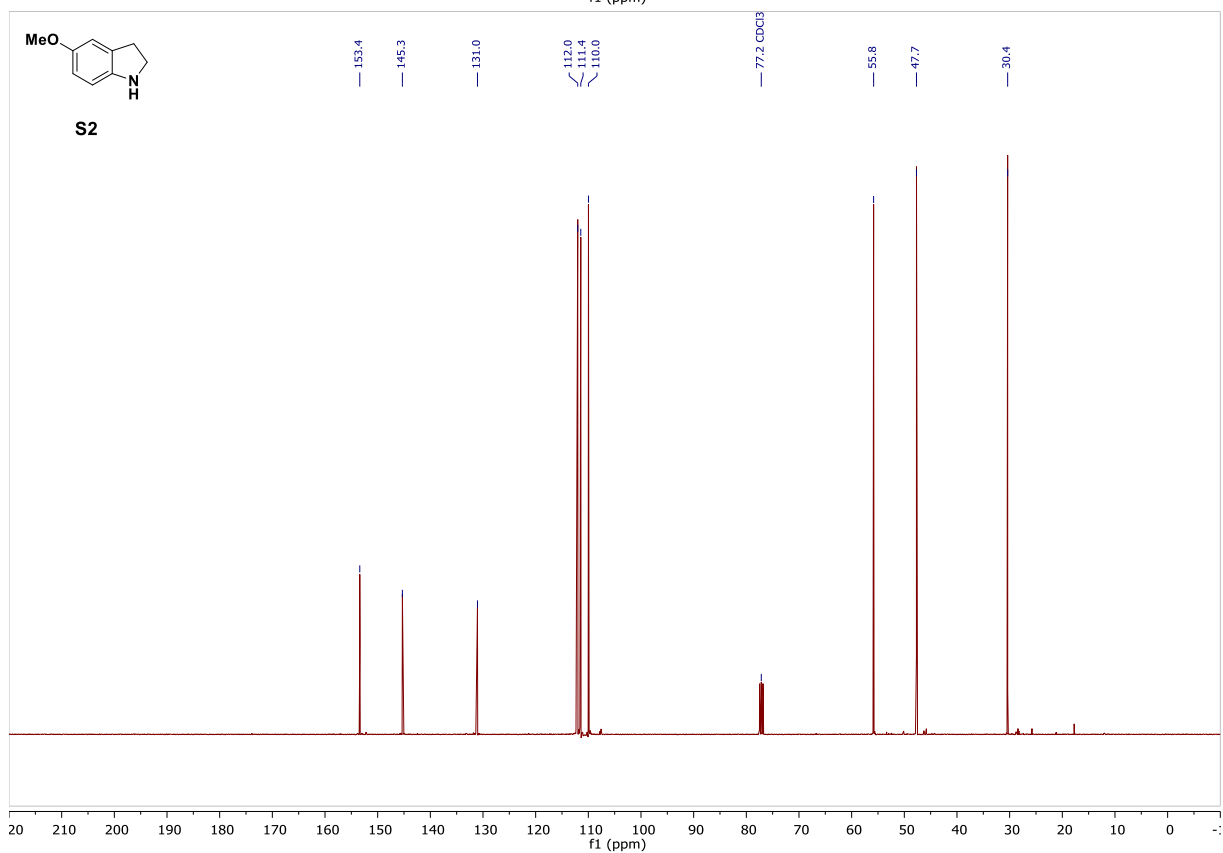
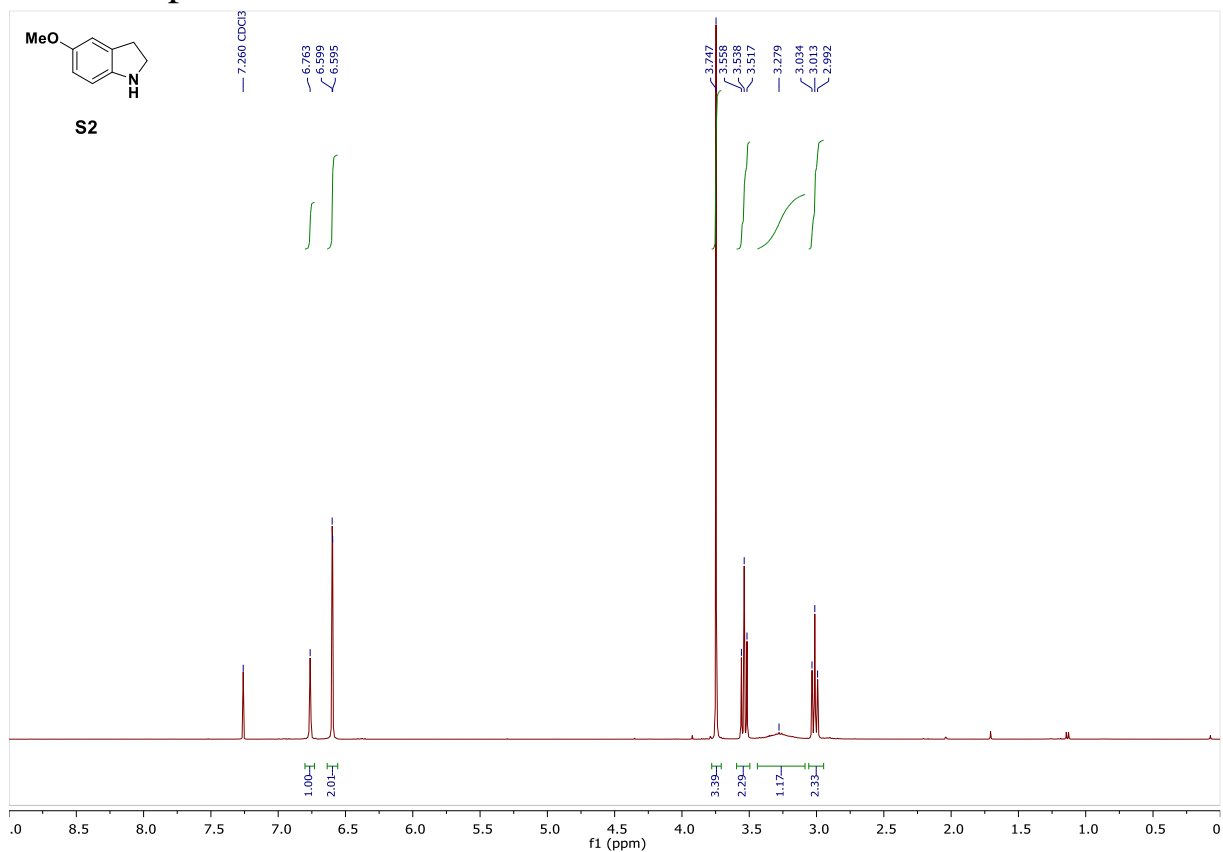
7.1 Compound S1



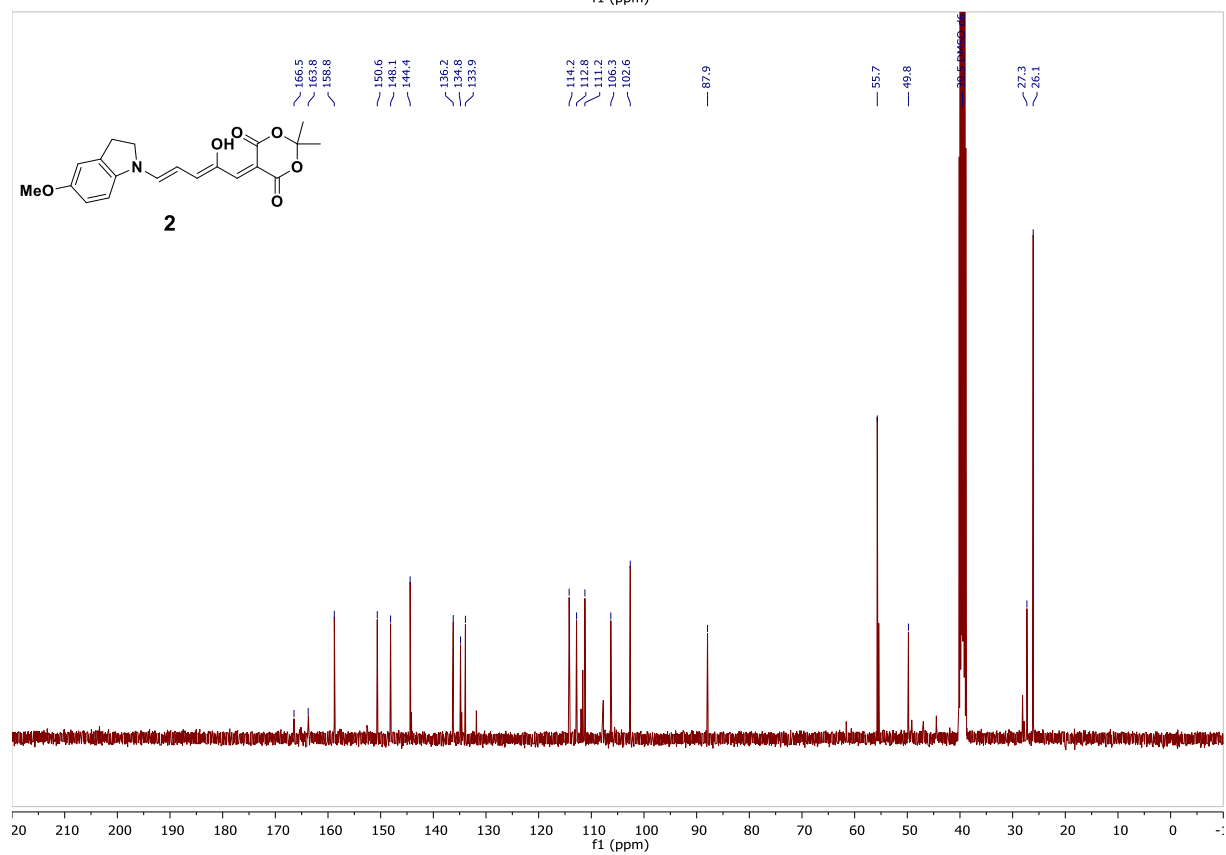
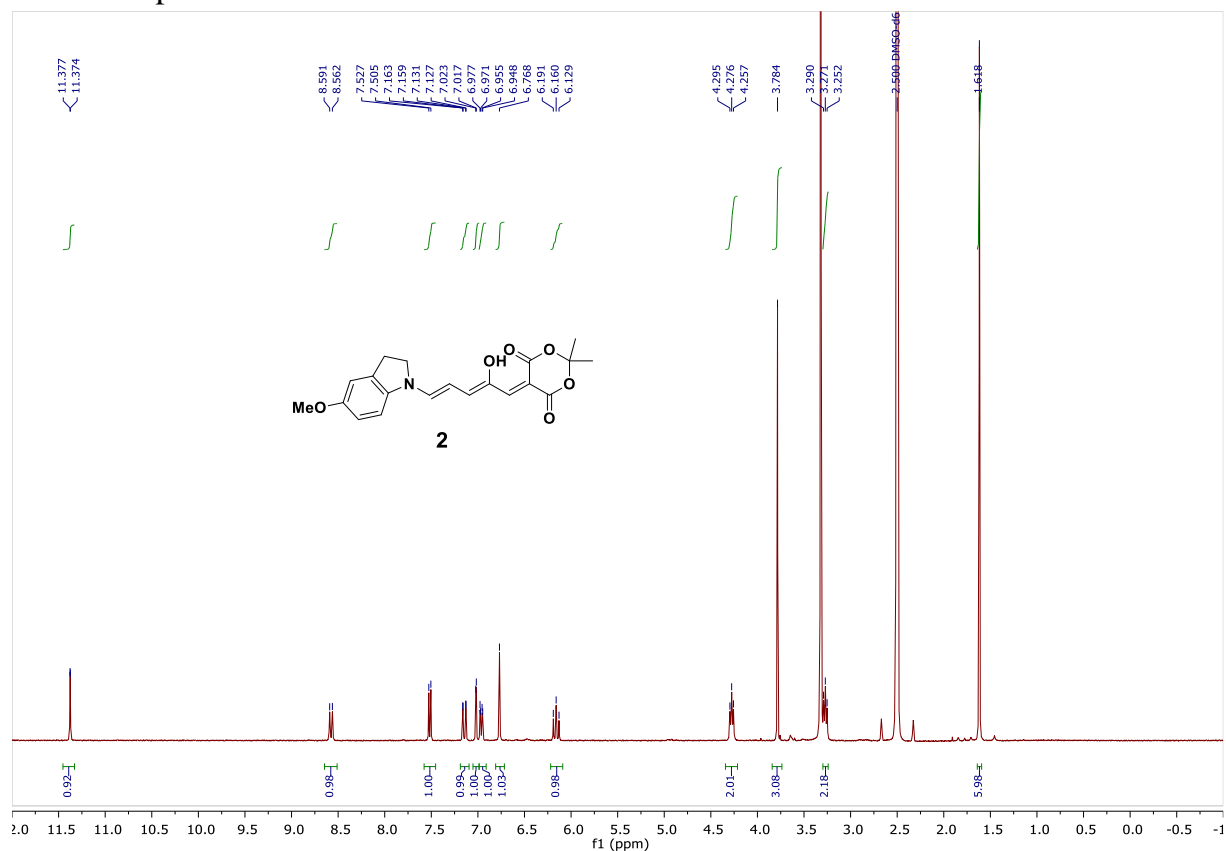
7.2 Compound 1



7.3 Compound S2



7.4 Compound 2



-
- (1) Pangborn, A. B.; Giardello, M. A.; Grubbs, R. H.; Rosen, R. K.; Timmers, F. J. *Organometallics* **1996**, *15*, 1518-1520.
 - (2) Seebach, D.; Imwinkelried, R.; Stucky, G. *Helv. Chim. Acta* **1987**, *70*, 448-464.
 - (3) Fulmer, G. R.; Miller, A. J. M.; Sherden, N. H.; Gottlieb, H. E.; Nudelman, A.; Stoltz, B. M.; Bercaw, J. E.; Goldberg, K. I. *Organometallics* **2010**, *29*, 2176-2179.
 - (4) Gentili, P. L.; Mugnai, M.; Bussotti, L.; Righini, R.; Foggi, P.; Cicchi, S.; Ghini, G.; Viviani, S.; Brandi, A., *J. Photochem. Photobiol. A*, **2007**, *187*, 209-221.
 - (5) Di Donato, M., Segado Centellas, M., Lapini A., Lima, M., Avila, F., Santoro, F. Cappelli, C., Righini, R., *J. Phys. Chem. B*, **2014**, *118*, 9613-9630.
 - (6) van Stokkum, I. H. M.; Larsen, D. S.; van Grondelle, R., *BBA - Bioenergetics* **2004**, *1657*, 82-104.
 - (7) a) Snellenburg, J. J.; Laptinok, S. P.; Seger, R.; Mullen, K. M.; van Stokkum, I. H. M., *J. Stat. Soft.* **2012**, *49*, 1-22.; b) Mullen, K. M.; van Stokkum, I. H. M., *J. Stat. Soft.* **2007**, *18*, 1-5.
 - (8) a) Henry, E. R., *Biophys. J.* **1997**, *72*, 652-673; b) Henry, E. R.; Hofrichter, J., *Meth. Enzymol.*, **1992**, *210*, 129-192.
 - (9) Lerch, M. M.; Wezenberg, S. J.; Szymanski, W.; Feringa, B. L. *J. Am. Chem. Soc.*, **2016**, *138*, 6344-6347.
 - (10) a) Helmy, S.; Leibfarth, F. A.; Oh, S.; Poelma, J. E.; Hawker, C. J.; Read de Alaniz, J. *J. Am. Chem. Soc.* **2014**, *136*, 8169-8172; b) Helmy, S.; Oh, S.; Leibfarth, F. A.; Hawker, C. J.; Read de Alaniz, J. *J. Org. Chem.* **2014**, *79*, 11316-11239.
 - (11) a) Johnson, K. F.; Van Zeeland, R.; Stanley, L. M. *Org. Lett.*, **2013**, *15*, 2798-2801; b) Gangjee, A; Vasudevan, A.; Queener, S. F. *J. Med. Chem.*, **1997**, *40*, 479-485.
 - (12) Hemmer, J. R.; Poelma, S. O.; Treat, N.; Page, Z. A.; Dolinski, N. D.; Diaz, Y. J.; Tomlinson, W.; Clark, K. D.; Hooper, J. P.; Hawker, C.; Read de Alaniz, J. *J. Am. Chem. Soc.*, **2016**, *138*, 13960-13966.
 - (13) Frisch, M. J. et al. *Gaussian09.D01*, Gaussian Inc. Wallingford, CT, **2009**.
 - (14) Frisch, M. J. et al. *Gaussian16.A03*, Gaussian Inc. Wallingford, CT, **2009**.
 - (15) Zhao, Y.; Truhlar D.G. *Theor Chem Account.* **2006**, *120*, 215-241.
 - (16) Ditchfield, R; Hehre, W.J; Pople, J. A., *J. Chem. Phys.*, **1971**, *54*, 724-728.
 - (17) Marenich, A.V.; Cramer, Ch. J.; Truhlar, D. J., *J. Phys. Chem. B*, **2009**, *113*, 6378-6396.
 - (18) a) Becke, A.D. *J. Chem. Phys.* **1993**, *98*, 5648-5652; b) Stephens, P.J.; Devlin, F.J.; Chabalowski, C.F.; Frisch, M.J. *J. Phys. Chem.* **1994**, *98*, 11623-11627.
 - (19) Ditchfield, R; Hehre, W.J; Pople, J. A., *J. Chem. Phys.* **1971**, *54*, 724-728.
 - (20) Barone, V.; Biczysko, M.; Bloino, J. *Phys Chem Chem Phys.* **2014** *16*, 1759-1787.
 - (21) Le Bahers, T.; Adamo, C.; Ciofini, I. *J. Chem. Theory Comput.* **2011**, *7*, 2498-2506; b) Jacquemin, D.; Le Bahers, T.; Adamo, C.; Ciofini, I. *Phys. Chem. Chem. Phys.* **2012**, *14*, 5383-5388.